

**EXPERIMENTAL INVESTIGATION OF HEAT TRANSFER
CHARACTERIZATION FOR CNT-NANOFLUID IN
HEAT EXCHANGERS**

BY

OSAMAH AWADH BIN DAHMAN

A Thesis Presented to the
DEANSHIP OF GRADUATE STUDIES

KING FAHD UNIVERSITY OF PETROLEUM & MINERALS

DHAHRAN, SAUDI ARABIA

In Partial Fulfillment of the
Requirements for the Degree of

MASTER OF SCIENCE

In

CHEMICAL ENGINEERING

JUNE 2011

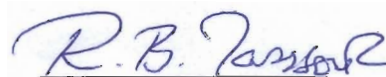
KING FAHD UNIVERSITY OF PETROLEUM AND MINERALS
DHAHRAN, SAUDI ARABIA
DEANSHIP OF GRADUATE STUDIES

This thesis, written by **Osamah Awadh Khamis Bin Dahman** under the direction of his thesis advisor and approved by his thesis committee, has been presented to and accepted by the Dean of Graduate Studies, in partial fulfillment of the requirements for the degree of **MASTER OF SCIENCE IN CHEMICAL ENGINEERING**.

Thesis Committee




Dr. Muataz A. Atieh
(Thesis Advisor)

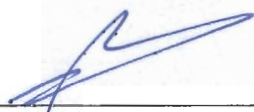


Dr. Rached Ben-Mansour

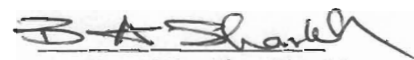
(Co-Advisor)



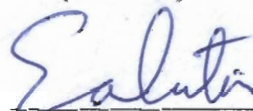
Dr. Usamah A. Al-Mubaiyedh
(Department Chairman)



Dr. Salam A. Zummo
(Dean of Graduate Studies)



Dr. Basel F. Abu-Sharkh
(Member)



Dr. Eid M. Al-Mutairi
(Member)



Dr. Mamdouh A. Al-Harathi
(Member)

30/5/11

Date

DEDICATION

This work is dedicated to my beloved **parents**, my **wife**, my **sisters** and my **son: *Hamza***

ACKNOWLEDGEMENTS

I really want to give my deepest gratitude to my advisor, *Dr. Muataz Ali Atieh*, for his support and confidence during the development of this study. I also want to thank *Dr. Rached Ben-Mansour*, my co-advisor, for his continuous supervision of the experimental works of this study. I also acknowledge my other committee members, *Prof. Basel Abu-Sharkh*, *Dr. Eid MUSAAD Al-Mutairi* and *Dr. Mamdouh Al-Harhi* for their constructive guidance, valuable advices and cooperation.

I am very grateful to *King Fahd University of Petroleum & Minerals (KFUPM)* and *King Abdul-Aziz City for Science and Technology (KACST)* for the opportunity to accomplish this work and for the financial support. I would like to thank all the KFUPM members and graduate students for the friendship they showed during the time of this study. Finally, all my gratitude to my family: my *father*, my *mother*, my *grandmother*, my *wife*, my *son* and my *sisters* for their love, patience, encouragement and prayers.

TABLE OF CONTENTS

TABLE OF CONTENTS	v
LIST OF TABLES	ix
LIST OF FIGURES	xi
ABSTRACT	xiv
THESIS ABSTRACT (ARABIC)	xv
CHAPTER ONE	1
1 INTRODUCTION	1
1.1 Background	1
1.2 Significance of Study	4
1.3 Potential Applications of Nanofluids.....	5
1.4 Objectives	6
CHAPTER TWO	7
2 LITERATURE REVIEW	7
2.1 Preparation of Nanofluids.....	7
2.1.1 <i>The Single-Step Method</i>	7
2.1.2 <i>The Two-Step Method</i>	8
2.2 Thermal Conductivity Enhancement in Nanofluids	11
2.3 Convection Heat Transfer in Nanofluids	16
CHAPTER THREE	28
3 EXPERIMENTAL METHODOLOGY	28
3.1 Materials	28

3.2	Functionalization of CNT	29
3.2.1	<i>Surface Oxidation of CNT</i>	29
3.2.2	<i>Functionalization of CNT with Polyethylene glycol</i>	32
3.2.3	<i>Functionalization of CNT with Dodecylamine</i>	33
3.2.4	<i>Functionalization of CNT with Octadecanol</i>	34
3.2.5	<i>Functionalization of CNT with Phenol</i>	35
3.3	Modification of CNT by Wet Impregnation Technique	36
3.3.1	<i>Steps of Metal Oxide Impregnation into the CNT Matrix</i>	36
3.4	Characterization	38
3.4.1	<i>Fourier Transform Infrared Spectroscopy (FTIR)</i>	38
3.4.1.1	<i>Samples Preparation</i>	39
3.4.2	<i>Thermal Analysis</i>	41
3.4.2.1	<i>Samples Preparation</i>	41
3.4.3	<i>Scanning Electron Microscopy (SEM)</i>	43
3.5	Preparation of Nanofluids	47
3.6	Measurement of Thermal Conductivity	48
3.7	Experimental Setup and Calculations	50
CHAPTER FOUR		54
4	RESULTS AND DISCUSSIONS	54
4.1	Characterization of Functionalized and Impregnated Carbon Nanotubes	54
4.1.1	Characterization of Functionalized Carbon Nanotubes by FTIR	54
4.1.1.1	<i>Acid Oxidized Carbon Nanotubes</i>	54
4.1.1.2	<i>Carbon Nanotubes Functionalized with Polyethylene Glycol</i>	56

4.1.1.3	<i>Carbon Nanotubes Functionalized with Dodecylamine</i>	58
4.1.1.4	<i>Carbon Nanotubes Functionalized with Phenol</i>	60
4.1.1.5	<i>Carbon Nanotubes Functionalized with Octadecanol</i>	62
4.1.2	Thermal Degradation Analysis of Functionalized Carbon Nanotubes	64
4.2	Characterization of Impregnated Carbon Nanotubes.....	71
4.2.1	<i>Scanning Electron Microscopy Images</i>	71
4.2.2	<i>Energy Dispersive X-ray Analysis</i>	71
4.3	Stability Study.....	76
4.4	Thermal Conductivity Measurements.....	79
4.4.1	Effect of Concentration on Thermal Conductivity at Different Temperatures. 79	
4.4.1.1	<i>Effect of Concentration on Thermal Conductivity for DI water+CNT-COOH Nanofluid</i>	79
4.4.1.2	<i>Effect of Concentration on Thermal Conductivity for DI water+CNT-PEG Nanofluid</i>	81
4.4.1.3	<i>Effect of Concentration on Thermal Conductivity for DI water+CNT-AL₂O₃ Nanofluid</i>	83
4.4.1.4	<i>Effect of Concentration on Thermal Conductivity for DI water+CNT-CuO Nanofluid</i>	85
4.5	Application of CNT-PEG Nanofluid in Heat Exchanger	87
CHAPTER FIVE		90
5	CONCLUSIONS AND RECOMMENDATIONS	90
5.1	Conclusions.....	90
5.2	Recommendations.....	91

APPENDIXE	92
REFERENCES.....	100
VITAE.....	106

LIST OF TABLES

Table 1.1 Thermal conductivity of different solids and liquids.....	3
Table 2.1 A list of the most frequently used models for effective thermal conductivity .	14
Table A4. 1 Thermal properties of CNT-COOH nanofluid at 35°C.....	92
Table A4. 2 Thermal properties of CNT-COOH nanofluid at 40°C.....	92
Table A4. 3 Thermal properties of CNT-COOH nanofluid at 45°C.....	92
Table A4. 4 Thermal properties of CNT-PEG nanofluid at 35°C.....	93
Table A4. 5 Thermal properties of CNT-PEG nanofluid at 40°C.....	93
Table A4. 6 Thermal properties of CNT-PEG nanofluid at 45°C.....	93
Table A4. 7 Thermal properties of CNT-10%CuO nanofluid at 35°C	94
Table A4. 8 Thermal properties of CNT-10%CuO nanofluid at 40°C	94
Table A4. 9 Thermal properties of CNT-10%CuO nanofluid at 45°C	94
Table A4. 10 Thermal properties of CNT-10%Al ₂ O ₃ nanofluid at 35°C	95
Table A4. 11 Thermal properties of CNT-10%Al ₂ O ₃ nanofluid at 40°C	95
Table A4. 12 Thermal properties of CNT-10%Al ₂ O ₃ nanofluid at 45°C	95
Table A4. 13 Experimental and calculated values for effectiveness calculations for water/water system.....	96
Table A4. 14 Experimental and calculated values for effectiveness calculations for 0.05 % CNT-PEG nanofluid in tube side and water in shell side.....	97
Table A4. 15 Experimental and calculated values for effectiveness calculations for 0.1 % CNT-PEG nanofluid in tube side and water in shell side	98

Table A4. 16 Experimental and calculated values for effectiveness calculations for 0.2 %
CNT-PEG nanofluid in tube side and water in shell side 99

LIST OF FIGURES

Figure 2.1 CNT nanofluids with and without dispersant:(a) CNTs quickly settle without using dispersant, and (b) CNTs are well dispersed and suspended in water by using a proper surfactant.	10
Figure 2.2 The experimental apparatus of Xuan and Li (2003).....	18
Figure 2.3 The experimental apparatus of Wen and Ding (2004)	19
Figure 2.4 The experimental apparatus of Yang et al. (2005)	22
Figure 2.5 The experimental apparatus of Heris et al. (2007)	25
Figure 2.6 The experimental apparatus of Asirvatham et al. (2009)	26
Figure 3.1 Acid modification of MWCNT through thermal oxidation	30
Figure 3.2 Photograph of functionalization process set up.....	31
Figure 3.3 Chemical modification of oxidized CNT with PEG.....	32
Figure 3.4 Chemical modification of oxidized CNT with dodecylamine.....	33
Figure 3.5 Chemical modification of oxidized CNT with octadecanol	34
Figure 3.6 Chemical modification of oxidized CNT with phenol	35
Figure 3.7 Photograph of Nicolet 6700 FTIR Spectrometer.....	40
Figure 3.8 Photograph of Netzsch model STA 449 F3 Jupiter® devise.....	42
Figure 3.9 Photograph of SEM JEOL 5800 LV Unit	46
Figure 3.10 Photograph of an ultrasonic cell disrupter.....	47
Figure 3.11 The Mathis TCi Thermal Conductivity Analyzer	48
Figure 3.12 Sensor face –diameter is 17 mm.....	49

Figure 3.13 Schematic layout of the experimental set up.....	52
Figure 3.14 Photograph of the experimental set up.....	53
Figure 4.1 FTIR spectra of oxidized CNT.....	55
Figure 4.2 FTIR spectra of CNT functionalized with polyethylene glycol.....	57
Figure 4.3 FTIR spectra of CNT functionalized with dodecylamine.....	59
Figure 4.4 FTIR spectra of CNT functionalized with phenol.....	61
Figure 4.5 FTIR spectra of CNT functionalized with octadecanol.....	63
Figure 4.6 TGA-DSC curves for modified carbon nanotubes with carboxylic group.....	66
Figure 4.7 TGA-DSC curves for modified carbon nanotubes with poly ethylene glycol group.....	67
Figure 4.8 TGA-DSC curves for modified carbon nanotubes with amine group.....	68
Figure 4.9 TGA-DSC curves for modified carbon nanotubes with octadecanoate group.....	69
Figure 4.10 TGA-DSC curves for modified carbon nanotubes with phenol group.....	70
Figure 4.11 SEM image of MWCNTs-CuO.....	72
Figure 4.12 SEM image of MWCNTs-AL ₂ O ₃	73
Figure 4.13 EDX pattern of MWCNTs-CuO.....	74
Figure 4.14 EDX pattern of MWCNTs-AL ₂ O ₃	75
Figure 4.15 Photographs of oxidized MWCNT and MWCNT-PEG nanofluid show no precipitation after two months.....	77
Figure 4.16 Photographs of impregnated MWCNT nanofluid show no precipitation in presence of SDS surfactant after two months.....	78
Figure 4.17 Thermal conductivity enhancement of DI water with CNT-COOH nanofluid.....	80

Figure 4.18 Thermal conductivity enhancement of DI water with CNT-PEG nanofluid	82
Figure 4.19 Thermal conductivity enhancement of DI water with CNT- Al_2O_3 nanofluid	84
Figure 4.20 Thermal conductivity enhancement of DI water and CNT-CuO nanofluid .	86
Figure 4.21 Effectiveness enhancement of CNT-PEG nanofluid in the turbulent regime	88
Figure 4.22 Effectiveness enhancement of CNT-PEG nanofluid in the laminar regime.	89

ABSTRACT

Full Name OSAMAH AWADH KHAMIS BIN DAHMAN
Title of Study EXPERIMENTAL INVESTIGATION OF HEAT TRANSFER CHARACTERIZATION FOR CNT-NANOFLUID IN HEAT EXCHANGERS
Major Field CHEMICAL ENGINEERING
Date of Degree JUNE 2011

A nanofluid is a suspension of ultrafine particles with extremely high thermal conductivity in a conventional base fluid which has the potential increases the heat transfer characteristics of the original fluid. Recently, newly developed material nanometer-sized particles have been utilized in suspension in conventional heat transfer fluids.

In this research work, multi-wall carbon nanotubes have been functionalized by different types of surfactant. In addition to that, two types of metal oxide nanoparticles have been impregnated on the surface of carbon nanotubes by using wet impregnation methods to enhance the thermal conductivity of the base fluids. The modified carbon nanotubes have been characterized by using Fourier Transfer Infrared (FTIR) and Thermogravimetric Analysis (TGA) as well as Scanning Electron Microscopy (SEM). The thermal conductivity has been measured using the Mathis TCi Thermal Conductivity Analyzer to study the effect of modified carbon nanotubes on the base fluids. The results show that, the CNT-PEG nanofluid has to be able to produce a stable nanofluid with deionized water for more than two months without visually observable precipitation. Also, CNT-PEG nanofluid shows more enhancements in thermal conductivity compared to the other tested nanofluids. The effectiveness of a concentric tube heat exchanger using CNT-PEG nanofluid was improved considerably by 25% at 0.2 wt % particle concentration.

THESIS ABSTRACT (ARABIC)

ملخص الرسالة

الإسم: أسامة عوض خميس بن دحمان

عنوان الرسالة: دراسة عملية لخصائص النقل الحراري باستخدام السوائل المحتوية على أنابيب الكربون النانوية في المبادلات الحرارية
التخصص: هندسة كيميائية

يعرف السائل النانوي بانه سائل يحتوي على دقائق متناهية الصغر (نانوية) لها موصلية حرارية عالية معلقة في سائل تقليدي والتي لها امكانية زيادة خصائص النقل الحراري للسائل الاصيل. حديثا إستعملت مواد جديدة متطورة ذات حجم نانوي كعوالق في سوائل نقل الحرارة التقليدية. في هذه الدراسة تم توظيف أنابيب الكربون النانوية بإضافة مجموعات وظيفية مختلفة وايضا تم تشييع سطح أنابيب الكربون النانوية باستخدام نوعين من اكاسيد المعادن بواسطة طريقة الاشباع الرطبة من اجل تحسين الموصلية الحرارية للسوائل. ولتميز المجموعات الوظيفية و اكاسيد المعادن على أسطح أنابيب الكربون النانوية تم استخدام مطياف الأشعة تحت الحمراء (FTIR) وتقنيات التحليل الحرارية (TGA) وتقني المجهر الالكتروني الماسح (SEM). ولقد تم استخدام جهاز قياس الموصلية الحرارية (Mathis TCi) لاجل دراسة تأثير أنابيب الكربون النانوية المعدلة على السوائل. أظهرت النتائج ان السائل النانوي المكون من الماء و أنابيب الكربون النانوية المعدلة باستخدام متعدد الايثيلين جلايكول قادر على انتاج سائل نانوي متجانس ومستقر لاكثر من شهرين من غير ترسيب. كما أظهر هذا السائل موصلية حرارية أكبر مقارنة مع بقية السوائل النانوية المختبرة الاخرى. كما أظهرت النتائج ان فعالية المبادل الحراري ذو الانابيب المتحدة المركز قد تحسنت لاكثر من % 25 عند استخدام السائل النانوي المكون من الماء و أنابيب الكربون النانوية المعدلة باستخدام متعدد الايثيلين جلايكول.

MASTER OF SCIENCE

KING FAHD UNIVERSITY OF PETROLEUM AND MINERALS

Dhahran, Saudi Arabia

June 2011

CHAPTER ONE

1 INTRODUCTION

1.1 Background

Various types of particles such as metallic, non-metallic and polymeric have been suspended into fluids to form suspensions containing millimeters or micrometer sized particles. However, they are not applicable for practical application due to problems such as sedimentation, erosion of pipelines, clogging of flow channels and increase in pressure drop due to their momentum transfer. Furthermore, they often suffer from rheological problems and instability. In particular, the particles tend to settle rapidly. However, these increase thermal conductivity but they are not of practical importance. A research group at Argonne National Laboratory was the first to continuously study the use of nano-sized particles around a decade ago.

A nanofluid is a suspension of ultra fine particles with extremely high thermal conductivity in a conventional base fluid which has the potential increases the heat transfer characteristics of the original fluid. Recently, newly developed material nanometer sized particles have been used in suspension in conventional heat transfer fluids.

Over the last several years, considerable research has been carried out leading to development of currently used heat transfer enhancement techniques. Generally, additives have been used to increase the heat transfer performance of the base fluid. Furthermore, these nanofluids are expected to ideally suited in practical application as their use incurs little or no penalty in pressure drop, change the transport properties and heat transfer characteristics of the base fluid. Due to ultra fine nature of these nanoparticles, nanofluids behave as a single phase fluid rather than multiphase, i.e., solid-liquid mixture.

Carbon nanotubes have generated great interest since they were discovered in 1991. The thermal conductivity of carbon nanotubes at room temperature is over 3,000 times greater than that of water and over 10,000 times greater than that of engine oil [1]. This large difference in thermal conductivity between liquids and carbon nanotubes is shown in Table 1.1 as compared to a variety of materials.

Table 1.1 Thermal conductivity of different solids and liquids [1]

Material	Form	Thermal Conductivity (W/m K)
Carbon	Nanotubes	1,800-2000
	Diamond	2,300
	Graphite	110-190
	Fullerenes(film)	0.4
Metallic Solids	Silver	429
	Copper	401
	Aluminum	237
	Nickel	158
Non-Metallic Solids	Silicon	148
	Alumina	40
Metallic Liquids	Sodium @ 644 K	72.3
Nonmetallic liquids	Water	0.613
	Ethylene Glycol	0.253
	Engine oil	0.145

Therefore, fluids containing suspended carbon nanotubes are expected to show significantly higher thermal conductivity compared with conventional heat transfer fluids. Carbon nanotubes, SWCNTs and MWCNTs have been found to considerably increase

the thermal conductivities of many heat transfer fluids such as synthetic oil, water, water/ethylene glycol mixtures and many other heat transfer fluids such as antifreeze. Prior Functionalization and mixing in appropriate solvents followed by homogenization and sonification were some of the methods used to achieve various levels of dispersions of CNTs in these fluids. CNTs are believed to contribute to the thermal conductivity of heat transfer fluids through Brownian motion and by formation of tri-dimensional network within the fluid. The preliminary evaluation of the viscosity of heat transfer nanofluids have the potential to find a place in many applications such as engine cooling systems, oil coolers and heat pumps to significantly increase their thermal and lubricating performance [1].

1.2 Significance of Study

Heat transfer fluids such as water, ethylene glycol, Freon and mineral oil play an important job in many industrial processes such as power generation, heating and cooling processes, chemical productions, transportations and microelectronics. The primary problem to the high compactness and effectiveness of the heat exchangers is the poor heat transfer characteristics of these fluids compared to solids. An improvement in thermal conductivity of these conventional fluids is a key idea to improve the heat transfer characteristics. Thus, the essential initiative is to seek solid particles especially nano-sized particles having thermal conductivity several thousand orders higher than those of conventional fluids. This study focuses on experimental investigation of heat transfer

characterization for CNT-nanofluid in heat exchanger taking into account various parameters such as dosage of CNT, type of metal oxide and type of surfactant.

1.3 Potential Applications of Nanofluids

Nanofluids could be used in many industrial sectors .The main applications of nanofluids can be highlighted as follow:

1. The use of nanofluids is expected to help the efforts to optimize the design of compact heat exchanging equipment.
2. Nanofluids can be used in wide variety of industries ranging from transportation industry, energy supply and production, textiles and paper industry by, for instance, decreasing pumping needs or reducing heat exchangers sizes.
3. Nanofluids can be used in pool boiling applications such as in electronics equipment cooling by enhancing the Critical Heat Flux (CHF).

1.4 Objectives

The main objectives of this research can be summarized as follows:

1. To functionalize the surface of CNTs by various surfactants as well as impregnated by different metal oxides.
2. To characterize the thermo-physical properties of nanofluids consisting of functionalized and impregnated multi-wall carbon nanotubes (MWCNT) suspended in a conventional working fluid (e.g. water).
3. To experimentally study the performance of nanofluids in a concentric tube heat exchanger and to compare that with conventional working fluids.

CHAPTER TWO

2 LITERATURE REVIEW

2.1 Preparation of Nanofluids

Preparation of nanofluids is the important step in the use of nanoparticles to improve the thermal conductivity of nanofluids. There are two main production techniques have been employed in producing nanofluids. One is a single-step method and the other is a two-step method.

2.1.1 The Single-Step Method

The single-step technique is a process combining the production of nanoparticles with the synthesis of nanofluids during one process cycle. Physical vapor deposition method (PVD) or chemical reduction technique can be used for preparing the nanoparticles. The processes such as drying, storage, transportation, and dispersion of nanoparticles into the base fluid are avoided in this method, therefore the agglomeration of nanoparticles is minimized and the stability of fluids is increased [2]. A single-step method is usually applied for metal nanofluid preparation. But the main disadvantages of this method are that only low vapor pressure fluids are compatible with the process and low concentration of nanoparticles. This limits the application of this method.

Eastman et al. [3] has used a one-step physical method to produce nanofluids, in which Cu vapor was directly condensed into nanoparticles by contact with a flowing low vapor

pressure liquid (ethylene glycol). Liu et al. [4] prepared nanofluids containing Cu nanoparticles in water through chemical reduction method for the first time. Lo et al. [5, 6] synthesized copper dioxide nanofluids by a single-step method called SANSS. The established SANSS demonstrated to be effective in avoiding particle aggregation and producing uniformly distributed and well-controlled size of CuO nanoparticles dispersed in a deionized water suspension. Zhu et al. [7] presented a novel one-step chemical method for preparing copper nanofluids by reducing copper sulfate pentahydrate with sodium hypophosphite in ethylene glycol under microwave irradiation. Nonagglomerated and stably suspended Cu nanofluids were synthesized.

2.1.2 The Two-Step Method

In the two-stage techniques, the nanoparticles are firstly prepared and then introduced into base fluid. Metal oxide nanoparticles, nanofibers or nanotubes used in this technique are first prepared as a dry powder by chemical vapor deposition (CVD), inert gas condensation, mechanical alloying or other suitable techniques, and the nanosized powder is then dispersed into a fluid in a second processing step. This step-by step method isolates the preparation of the nanofluids from the preparation of nanoparticles. Consequently, agglomeration of nanoparticles due to attractive Vander Waals Forces may occur in both steps, especially in the process of drying, storage, and transportation of nanoparticles [2]. The agglomeration will not only cause the settlement and clogging of microchannels, but also decrease the thermal conductivity. Several techniques such as use of ultrasonic agitation equipment, pH control or addition of stabilizers to the fluids are often applied to minimize particle aggregation and improve dispersion behavior. Since nanopowder synthesis techniques have already been scaled up to industrial production

levels by several companies, there are prospective economic advantages in using two-step synthesis techniques that depend on the use of such powders. But an important problem that needs to be solved is the stabilization of the suspension prepared. Figure 2.1 shows two kinds of CNT nanofluids with and without adding stabilizer.

Liu [8] and Choi [9] produced carbon nanotube suspensions by a two-step method. In order to avoid the agglomeration of carbon nanoparticles, surfactants and ultrasonic agitation were used. Hong et al. [10,11] produced Fe nanofluids by dispersing Fe nanocrystalline powder in ethylene glycol by a two-step method. The Fe nanoparticles with a mean size of 10 nm were synthesized by a chemical vapor condensation process (CVD). To avoid the agglomeration of nanoparticles in nanofluids, they used an ultrasonic cell disrupter generating ultrasonic pulses of 700W at 20 kHz. Xuan et al. [12,13,14] prepared Cu/ H₂O, Cu/oil nanofluids by two-step method. In order to avoid nanoparticle congregating, surfactants and ultrasonic agitation were used. Murshed et al. [15] presented TiO₂ suspension in water prepared by two-step method. Xie et al. [16] prepared Al₂O₃/H₂O, Al₂O₃/EG, Al₂O₃/ PO nanofluids by two-step method, and intensive ultrasonication and magnetic force agitation were utilized to avoid nanoparticle aggregation.

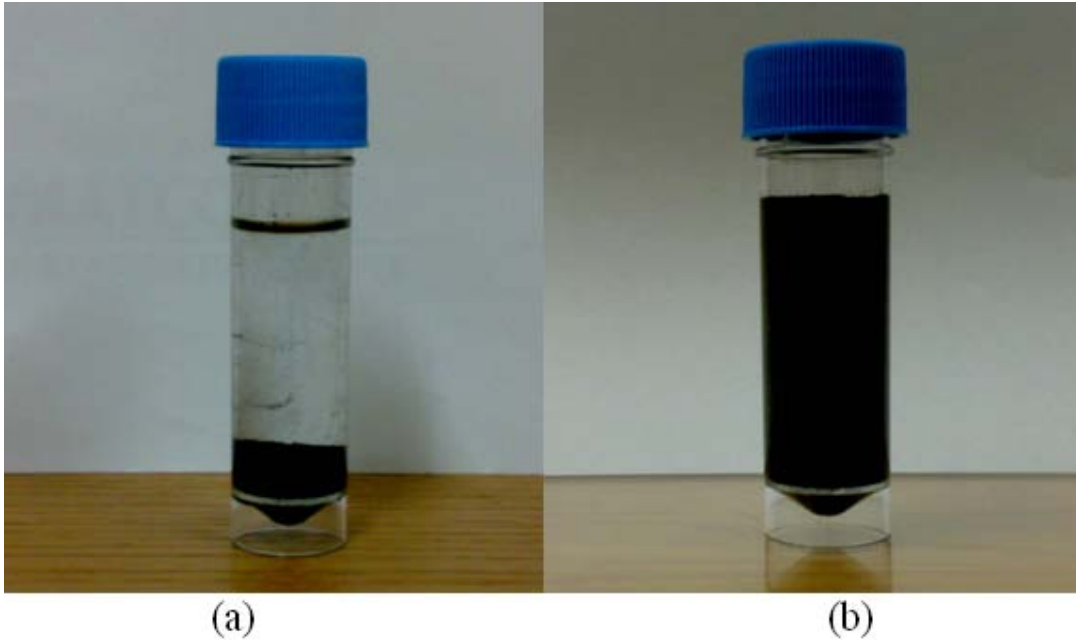


Figure 2.1 CNT nanofluids with and without dispersant:(a) CNTs quickly settle without using dispersant, and (b) CNTs are well dispersed and suspended in water by using a proper surfactant.

2.2 Thermal Conductivity Enhancement in Nanofluids

Thermal conductivity is the most important parameter responsible for enhancing heat transfer performance of a heat transfer fluid; therefore many experimental works have been reported on this aspect. The transient hotwire method was found to be more suitable compared to other steady-state-parallel-plate techniques and temperature oscillation techniques because in general nanofluids are electrically conductive and it is difficult to apply other methods directly.

Lee et al. [17] measured thermal conductivity of four oxide nanofluids (Al_2O_3 in water, Al_2O_3 in ethylene glycol, CuO in water, and CuO in ethylene glycol) by a transient hot-wire method at room temperature. They used volume fractions of 1% to 5%. They found that the thermal conductivity enhancement of the Al_2O_3 and CuO nanofluids were high and the enhancement was higher when ethylene glycol was the base fluid. An enhancement of 20% was observed at 4% volume fraction of CuO . Also, they noticed that, the enhancement when water was the base fluid was lower but still substantial, with 12% enhancement at 3.5% CuO , and 10% enhancement with 4% Al_2O_3 .

Eastman et al. [18] measured thermal conductivity of three nanofluids of copper nanometer-sized particles suspended in ethylene glycol by a transient hot-wire technique. The first containing old copper particles (prepared and stored for a period of time) in ethylene glycol. In the second nanofluid the particles were used directly after preparation. In the third group a small quantity of thioglycolic acid was added to improve the stability of the metal particles against settling. They found that the effective thermal conductivity of ethylene glycol containing approximately 0.3 vol % Cu nanoparticles of mean diameter < 10 nm in presence of thioglycolic acid as a dispersant was increased by 40%.

The highest improvement on the thermal conductivity of nanofluids that was reported in the literature was the work of Choi et al. at Argonne National Laboratory (ANL) [19]. They found that the nanofluid of multi-walled carbon nanotubes (MWCNTs) of about 25 nm mean diameter and 50 μm average length suspended in engine oil showed a phenomenal 160 % increase in thermal conductivity with just 1% volume fraction of the nanotubes. Choi et al used a transient hotwire method for the thermal conductivity measurement.

Assael et al. [20] measured thermal conductivity of suspension of multi-walled CNTs of about 25 nm inner diameter in water. Sodium dodecyl sulfate (SDS) was employed as a dispersant. The transient hotwire technique was used for the thermal conductivity measurement. Their study indicated that the maximum enhancement of the thermal conductivity was 38 % obtained for a 0.6 vol % suspension of MWCNTs and water with SDS.

Assael et al. [21] also measured thermal conductivity of multi-walled as well as double walled CNTs suspended in water at ambient temperature. Hexadecyltrimethyl ammonium bromide (CTAB) and Nanospense AQ were employed as dispersants. They found that the thermal conductivity enhancement of MWCNTs of around 130 nm average diameter and 40 μm average length suspension in water with (CTAB) was 34 % for 0.6 % volume whereas that of double walled CNTs was found to be 7.6 % for 1 % volume suspension in water with (CTAB).

Liu et al. [22] measured thermal conductivity of MWCNTs of 20 to 50 nm in diameter suspend in ethylene glycol and engine oil with a modified transient hot wire method at room temperature. No surfactant was used in carbon nanotube–ethylene glycol

suspensions. On the other hand, N-hydroxysuccinimide (NHS) was employed as the dispersant in carbon nanotube synthetic engine oil suspensions.

They noticed an increase of 12.4 % in the thermal conductivity of CNT suspension in ethylene glycol for 1 % volume fraction while 30% enhancement in the CNT suspension in synthetic oil for 2 % volume fraction.

Hwang et al. [23] measured thermal conductivity of four kinds of nanofluids such as multiwalled carbon nanotube (MWCNT) in water, CuO in water, SiO₂ in water, and CuO in ethylene glycol by a transient hot wire method. Since MWCNTs are entangled and agglomerated in aqueous suspension, sodium dodecyl sulfate (SDS) was used as a surfactant when producing MWCNT nanofluids. Their results showed that the thermal conductivity enhancement of water-based MWCNT nanofluid was increased up to 11.3% at a volume fraction of 0.01. Their results also showed that the thermal conductivity of nanofluids depends on the thermal conductivity of the suspended particles and base fluids.

The effective thermal conductivity can be calculated with predicted models. Maxwell was one of the first to analytically investigate conduction through suspended particles. This model and other models for thermal conductivity e.g., Hamilton and Crosser, and Jeffrey predict thermal conductivity reasonably well for dilute mixtures of relatively large particles in fluids. However, so far no model can be generally utilized to predict the enhancing effects in thermal conductivity of different nanofluids. Table 2.2 shows different macroscopic models proposed for suspensions and composite materials [24].

Table 2.1 A list of the most frequently used models for effective thermal conductivity

Model	Expressions	Remarks
Maxwell (1873)	$\frac{K_{eff}}{K_L} = \frac{K_s + 2K_L + 2(K_s - K_L)\phi_s}{K_s + 2K_L - (K_s - K_L)\phi_s}$	Spherical particles ϕ_s – solids volume fraction
Hamilton & Crosser (1962)	$\frac{K_{eff}}{K_L} = \frac{K_s + (n-1)K_L - (n-1)\phi_s(K_L - K_s)}{K_s + (n-1)K_f + \phi_s(K_L - K_s)}$	n depends on particle shape and K_s/K_L , $n=3/\psi$ for $K_s/K_L \gg 100$, $n=3$ for other cases, ψ - sphericity
Jeffrey (1973)	$\frac{K_{eff}}{K_L} = 1 + \frac{3\phi_s(K_s/K_L - 1)}{K_s/K_L + 2} + 3\phi_s^2 \left(\frac{K_s/K_L - 1}{K_s/K_L + 2}\right)^2 \cdot \left[1 + \frac{1}{4} \left(\frac{K_s/K_L - 1}{K_s/K_L + 2}\right) + \frac{3}{16} \left(\frac{K_s/K_L - 1}{K_s/K_L + 2}\right) \left(\frac{K_s/K_L + 2}{2K_s/K_L + 3}\right) + \dots\right]$	High order terms represent pair interactions of randomly dispersed particles
Davis (1986)	$\frac{K_{eff}}{K_L} = 1 + \frac{3(K_s/K_L - 1) \cdot [\phi_s + f \cdot \phi_s^2 + O(\phi_s^3)]}{(K_s/K_L + 2) - (K_s/K_L - 1)\phi_s}$	High order terms due to pair interactions of randomly dispersed spheres, $f=2.5$ & 0.5 for $K_s/K_L=10$ and ∞ , respectively
Bruggeman (1935)	$\frac{K_{eff}}{K_L} = [(3\phi_s - 1)\frac{K_s}{K_f} + (2 - 3\phi_s) + \sqrt{\Delta}]/4$ $\Delta = (3\phi_s - 1)^2(K_s/K_L)^2 + (2 - 3\phi_s)^2 + 2(2 + 9\phi_s - 9\phi_s^2)(K_s/K_L)$	Spherical particles, interactions between particles considered, applicable to high concentrations

In the last few years, many efforts have been made to predict the enhancement in thermal conductivity of CNT nanofluids by different assumptions like fractal theory, liquid layering etc. Xue [25] presented a model for thermal conductivity of CNT nanofluids using field factor approach, with a depolarization factor and an effective dielectric constant. The model is found to be working fairly well in predicting the thermal

conductivities of CNT nanofluids. Nan et al. [26] reported a simple formula for thermal conductivity enhancement in CNT composites which is derived from the Maxwell-Garnett model by the effective-medium approach. The model over-predicts the enhancement in the thermal conductivity of CNT suspensions when calculated with typical values of CNT thermal conductivities. Nan et al. [27] also developed a new model by incorporating interface thermal resistance with an effective-medium approach. However, the model needs the thermal resistance value at the surface of CNTs, which is difficult to obtain for different types of CNTs and their combinations with different base fluids. Recently, Gao and Zhou [28] reported another model derived from the Maxwell-Garnett model, based on differential effective medium theory. The model proposed a non-linear dependence of thermal conductivity of CNT nanofluids over volume concentration of the carbon nanotubes, with slow increase at low concentrations and rapid at high concentrations. There are some more models have been reported to predict the enhancing effects in thermal conductivity of different CNT nanofluids, but none of them conform to the experimental observations, for all the available experimental results.

2.3 Convection Heat Transfer in Nanofluids

The thermal conductivity enhancement in nanofluids only provides a necessary condition for its application; the satisfactory condition comes from the proof of the performance of these fluids in convective environments.

The convective heat transfer of nanofluids has attracted comparatively slight attention in literature. There are few studies dealing with the convection heat transfer in nanofluids. The most productive works have been done by the following researchers.

Pak and Cho [29] studied the heat transfer performance of two different metallic oxide particles, $\gamma\text{-Al}_2\text{O}_3$ (13 nm) and TiO_2 (27nm), in water based nanofluids in a circular pipe. The Reynolds and Prandtl numbers varied in the ranges $10^4\text{-}10^5$ and 6.5-12.3, respectively. They found that the Nusselt number for the dispersed fluids of the volume concentration ranged from 1% to 3% for fully developed turbulent flow increased with increasing volume concentration as well as the Reynolds number. However, it was found that the convective heat transfer coefficient of the dispersed fluid at a volume concentration of 3 % was 12% lower than that of pure water for a constant average velocity. The possible reason was that the suspensions have higher viscosity than that of pure water, especially at high particle volume concentration.

Eastman et al. [30] carried out heat transfer tests to investigate the thermal performance of nanofluids consisting of copper oxide nanoparticles dispersed in water under dynamic flow conditions. They found that, at fixed flow rates, the heat transfer coefficient of water containing less than 1 vol. % of CuO nanoparticles was improved by more than 15 % when compared with pure water.

Xuan and Li [31] presented an experimental system to investigate the convective heat transfer coefficient and friction factor of nanofluids for turbulent flow in a tube. The sample nanofluid used in this study was deionized water with a dispersion of Cu particles with less than 100nm diameter. The nanofluids, with different particle volume percentages, were used to determine the effect of the nanoparticle concentration on the heat transfer coefficient, the percentages being 0.3%, 0.5%, 0.8%, 1%, 1.2%, 1.5% and 2%. The Reynolds number of the nanofluids varied within the range of 10000–25,000. The experimental apparatus was mainly composed of a reservoir tank, a pump, a pipeline, a test section, a cooler, and a fluid collection tank. The test section was a straight brass tube of the inner diameter of 10 mm and the length of 800 mm. To obtain a constant wall heat flux boundary condition, the heat transfer section was heated electrically by a DC power supply capable of delivering a maximum of a 3.5 kW.

To prevent the aggregation of the nanoparticles in the base fluid, a fatty acid was used as a dispersant to cover the nanoparticles. The experimental apparatus of their work is depicted in Figure 2.2.

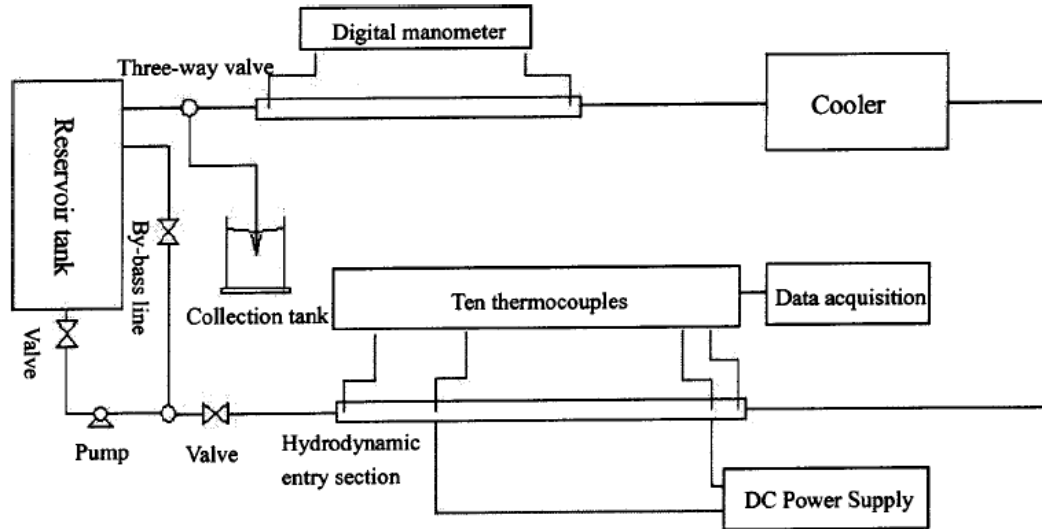


Figure 2.2 The experimental apparatus of Xuan and Li (2003)

The experimental results showed that the suspended nanoparticles remarkably enhanced heat transfer process and the nanofluid has larger heat transfer coefficient than that of the original base fluid under the same Reynolds number. Compared with water, the Nusselt number of the nanofluid with 2 % volume fraction of Cu particles was 39 % higher. It was also found that the friction factor for the nanofluids at low volume fraction did not produce an extra penalty in the pumping power.

Wen and Ding [32] presented an experimental study which evaluated the convective heat transfer coefficient of $\gamma\text{-Al}_2\text{O}_3$ particles with a size range of 27-56 nm, suspended in deionized water for laminar flow in a copper tube, focusing in particular on the entrance region. The various concentrations of nanoparticles (0.6%, 1.0%, and 1.6%) were tested under a constant wall heat flux. The experimental system constructed for this work is shown schematically in Figure 2.3. It consisted of a flow loop, a heating unit, a cooling part, and a measuring and control unit. The flow loop included a pump with a built-in

flow meter, a reservoir, a collection tank and a test section. A straight copper tube with 970mm length, 4.5 mm inner diameter, and 6.35 mm outer diameter was used as the test section. A 300W silicon rubber flexible heater was used to keep a constant heat flux boundary condition. A peristaltic pump was used to deliver a maximum flow rate of 10 l/min. The flow rate was controlled by adjusting rotational speed of the pump. In order to stabilize the nanoparticles, sodium dodecylbenzene sulfonate (SDBS) was used as a dispersant.

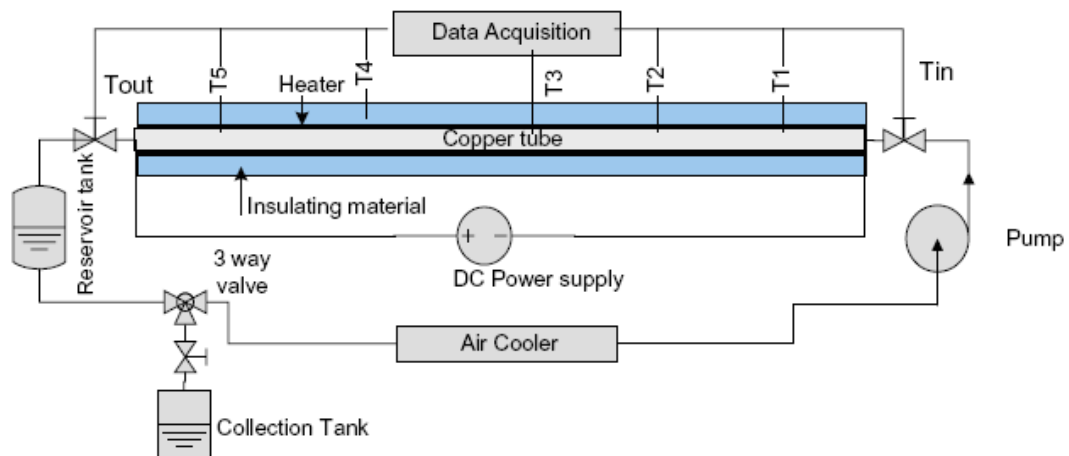


Figure 2.3 The experimental apparatus of Wen and Ding (2004)

The results showed considerable enhancement of convective heat transfer coefficient in the laminar flow regime, and enhancement increased with Reynolds number, as well as particle concentration. The enhancement was particularly significant in the entrance region, and decreased with axial distance.

Particle migration was proposed to be a reason for the enhancement, which results a non-uniform distribution of thermal conductivity and viscosity field and reduces the thermal boundary layer thickness.

Ding et al. [33] investigated the heat transfer performance of multi-walled carbon nanotube nanofluids in a straight copper tube. Distilled water and multi-walled carbon nanotubes were used to produce nanofluids. The experimental system constructed for this work is similar to that one used by Wen and Ding [32].

They found that the effective thermal conductivity increased with increasing temperature and CNT concentration. At a given shear rate, the viscosity of nanofluids increased with increasing CNT concentration and decreasing temperature. The presence of carbon nanotubes increased the convective heat transfer coefficient significantly, and the increase was more considerable at high CNT concentrations. It was also found that the convective heat transfer coefficient increased with increasing Reynolds number and the maximum enhancement was observed over 350 % at $Re = 800$ for 0.5 wt.% CNTs and the convective heat transfer coefficient at $pH = 6$ was slightly higher than that at $pH = 10.5$.

Particle re-arrangement, shear-induced thermal conduction enhancement, a reduction of the thermal boundary layer thickness due to the presence of nanoparticles, and the very high aspect ratio of CNTs were suggested as possible reasons of enhanced convective heat transfer.

Yang et al. [34] investigated experimentally the convective heat transfer performance of graphite nanoparticles with 1-2 μm average diameter and with the thickness around 20-40 nm, dispersed in liquid for laminar flow in a horizontal tube heat exchanger.

Nanoparticles of different sources were used in this study and focused on an aspect ratio (l/d) of about 0.02 (like a disc), to avoid the considerable increase in viscosity because the addition of large aspect ratio particles into a fluid. In this study, two types of nanofluids with different base fluids were used.

The experiments were performed within the following ranges: the volume flow rates were between 62–507 cm^3/min that gave average linear velocity between 6.3 and 52 cm/sec , the Reynolds number varied between 5–110, and the heating fluid temperature between 50–70°C. This work aimed to study the effects of the Reynolds number, volume fraction, temperature, nanoparticle source, and type of base fluid on the convective heat transfer coefficient. The experimental system used in this study is shown schematically in Figure 2.4.

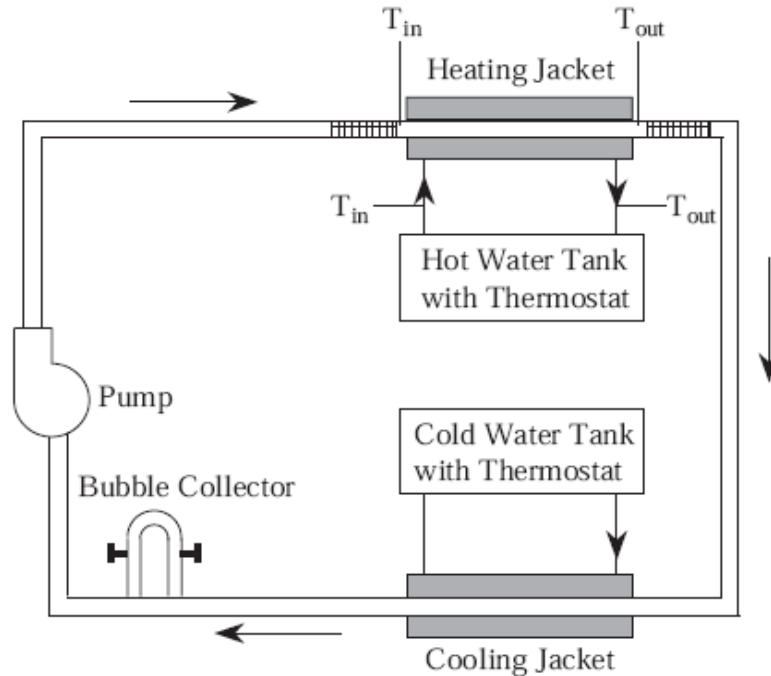


Figure 2.4 The experimental apparatus of Yang et al. (2005)

The entire system was heavily insulated to reduce heat loss. Pipes were wrapped with insulation material, and plastic fittings were attached at both ends of the test area to thermally isolate the connection. Static mixers were put at the ends of the test section to mix the fluids and improve accuracy of the bulk fluid temperature measurement. Appositive displacement pump was used to control the fluid flow rate and the bubble collector was used to collect and separate air bubbles from the fluid.

The experimental results showed that the heat transfer coefficient increased with the Reynolds number and the particle volume fraction in laminar flow. For example, at 2wt% the heat transfer coefficient of the nanofluids was moderately increased compared with the base fluid, but at 2.5 wt% it was 22% higher than the base fluid at 50 °C fluid temperature and 15% higher at 70 °C. Two factors were proposed to smaller improvements in heat transfer enhancement of nanofluids with increased fluid

temperature. One was the rapid alignment of nanoparticles in less viscous fluids, leading to less contact between the nanoparticles. The other factor was the depletion of particles in the near-wall fluid phase could lead to a lower thermal conductivity layer near the wall. Also, the experimental results showed that two graphite nanoparticle sources at same particle loading gave different heat transfer coefficient. Particle shape, morphology and surface treatment were suggested to be reasons for this behavior.

Heris et al. [35] investigated experimentally the convective heat transfer of nanofluids. The sample nanofluid used in this study was Al_2O_3 nanoparticles with an average diameter of 20 nm dispersed in distilled water with different concentrations including 0.2%, 0.5%, 1.0%, 1.5%, 2.0% and 2.5% volume fraction in laminar flow through circular tube with constant wall temperature boundary condition.

The experimental set-up consisted of a flow loop containing several sections such as temperature, pressure and flow rate measuring units, heating and cooling sections and flow controlling system. A two liter glass vessel equipped by drain valve was used as fluid reservoir. In order to control the fluid flow rate a reflux line with a valve was used. The test section consisted of 1 m annular tube which was constructed of 6 mm diameter inner copper tube with 0.5 mm thickness and 32 mm diameter outer stainless steel tube. Nanofluid flowed inside the inner tube while saturated steam entered annular section, which created constant wall temperature boundary condition. A steam trap was installed in vapor exiting line. The outer tube was insulated by fiber glass. The experimental apparatus of their work is depicted in Figure 2.5.

The experimental results showed that heat transfer coefficient of nanofluids increased with Peclet number as well as nanoparticles concentration. The increase in heat transfer

coefficient due to presence of nanoparticles was much higher than the prediction of single phase heat transfer correlation used with nanofluid properties. It was concluded that the thermal conductivity increase was not the only reason for heat transfer enhancement in nanofluids. Other factors such as dispersion and chaotic movement of nanoparticles, Brownian motion and particle migration were proposed to play an important role in heat transfer enhancement.

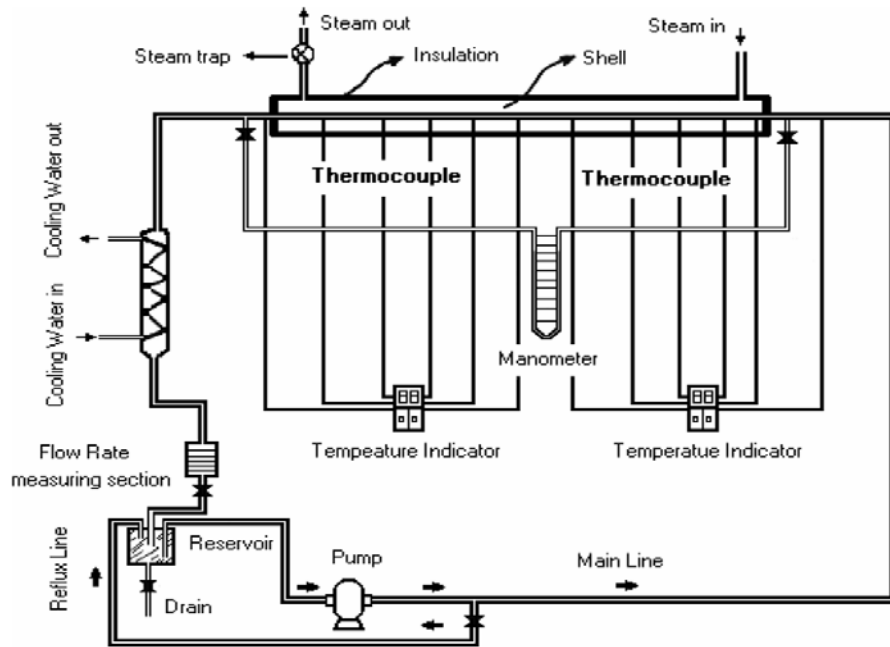


Figure 2.5 The experimental apparatus of Heris et al. (2007)

Asirvatham et al. [36] studied experimentally the steady state convective heat transfer of nanofluid of copper oxide (CuO) nanoparticles with an average diameter of 40 nm dispersed in de-ionized water with a low volume fraction (0.003% by volume) under laminar flow condition.

Experiments were performed for mass flow rates ranged from 0.0113 kg/s to 0.0139 kg/s and inlet temperatures at 10°C and 17°C and Reynolds number from 1,350 to 2,170.

The experimental setup is shown in Figure 2.6. It consisted of a test section which was 8 mm copper tube of 1,500 mm length with a tape heater (1 kW) wound around its lateral surface. The copper tube was well insulated with ceramic glass wool to avoid any heat leakage. Eight thermocouples (T-type) were fixed on the surface of the tube at 17 cm intervals to measure the change in surface temperature when the nanofluid receives heat from the heater. There were two pressure transducers at the inlet and outlet to measure

the pressure drop across the test section. The hot fluid pumped from the test section was cooled by an auxiliary cooling system with temperature controller. The pump used in this work was a centrifugal type capable of delivering a maximum flow rate of 200 LPH. The flow rate of fluid was regulated by operating the valves in the discharge line of the pump with corresponding adjustment in the bypass valve too. The flow rate could be measured by the flow meter. All the temperature and pressure sensors were connected to a data acquisition.

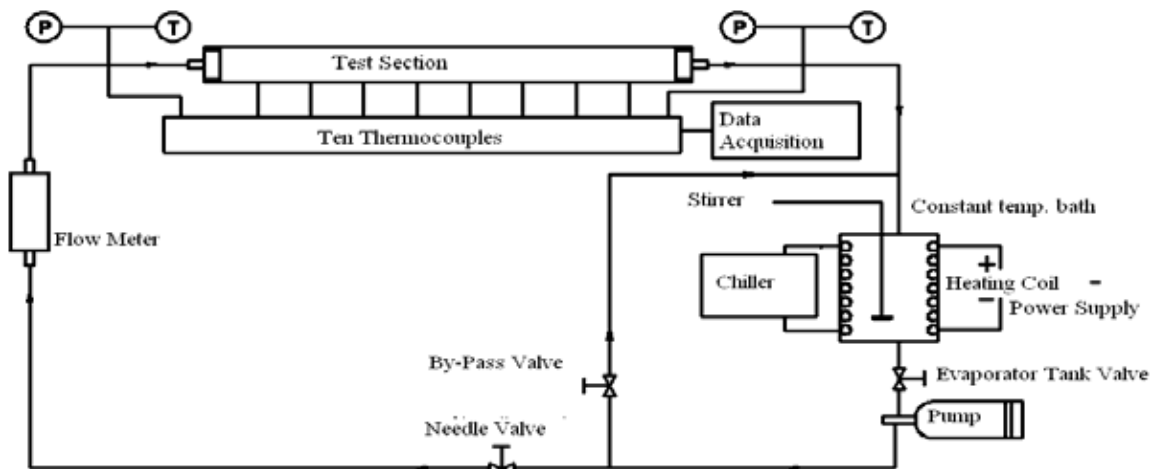


Figure 2.6 The experimental apparatus of Asirvatham et al. (2009)

They found that the existence of nanoparticles increased the convective heat transfer coefficient by 8 % than that of the original base fluid under the same Reynolds number; and the increase was significant even though the concentration was less. They also found that at a given concentration the enhancement of heat transfer coefficient increased in the entrance region and decreased with the axial distance.

The thermo-physical properties of nanofluids and chaotic movement of ultrafine particles were considered to be the important factors for the increase in heat transfer rate.

CHAPTER THREE

3 EXPERIMENTAL METHODOLOGY

In this chapter, various methods to be used in the experimental works are described in details. This includes the functionalization of CNT surface using different surfactants, impregnation of CNT surface using different metal oxides, preparation of nanofluids using those functionalized and impregnated CNTs, measuring the thermal conductivity using the modified transient plane source technique as well as the various characterization techniques. Also in this chapter, the experimental set up for studying the effectiveness of heat exchanger is described in details.

3.1 Materials

The multiwalled carbon nanotubes were purchased from Nanostructured and Amorphous Materials Inc, USA .The MWCNT is 8-15 nm in diameter and 10–50 μm in length with 230 m^2/g specific area. The purity of MWCNT is 95%. The carbon nanotubes were used without further purification. Four commercial surfactants, PEG20000 (Fluka with 98% purity), 1-octadecanol (Merck, 97% purity), phenol (Aldrich, 98% purity) and dodecylamine (Merck, 97% purity), were used for functionalizing carbon nanotubes.

3.2 Functionalization of CNT

Over the past decade, carbon nanotubes (CNTs) have received significant attention from many researchers because of their interesting properties and broad applications. In addition to their excellent mechanical characteristics, CNTs show unique electrical and thermal properties. These advanced properties provide exciting opportunities to produce newly develop materials for various applications. In this research functionalized CNTs have been used to improve the thermal conductivity of heat transfer fluids.

In this work, the functionalized MWCNTs obtained using different functional groups are prepared using the Fischer Esterification method.

The Fischer Esterification is an equilibrium reaction, whereas other esterification routes do not involve equilibrium. To shift the equilibrium to favor the production of esters, it is customary to use an excess of one of the reactants, either the alcohol or the acid. In the present reactions, an excess of the phenol, dodecylamine, 1-octadecanol, and polyethylene glycol have been used. Another way to drive a reaction toward its products is to remove water formed in this reaction by evaporation during the reaction [37].

3.2.1 Surface Oxidation of CNT

The most reported method of oxidizing the surface of carbon nanotubes is through acid treatment. It usually involves the use of concentrated strong acids such as sulfuric and nitric acid. Such way leads to the removal of the catalysts from carbon nanotubes and opening the tube caps as well as and formation of holes in the sidewalls, followed by an oxidative etching along the walls with the concomitant release of carbon dioxide [37].

In this work, As-received MWCNTs were added into a concentrated nitric acid (69%, AnalaR grade) in a ratio 1g: 10ml in a 500 ml three-necked flask equipped with mechanical stirrer and reflux condenser. The mixture was refluxed under constant agitation at 120 °C for 48 hours. Figure 3.1 gives the reaction mechanism for the oxidation of CNT.

After cooling to room temperature, the acid modified MWCNTs was thoroughly washed several times with deionized water to remove any un-reacted acid until the pH around 7 followed by filtration through a filter paper (3µm porosity).The acid modified MWCNTs, was then dried in a vacuum oven at 80 °C for 24 hours and crushed.

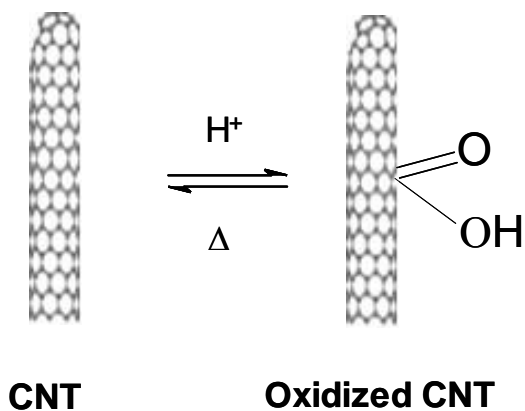


Figure 3.1 Acid modification of MWCNT through thermal oxidation



Figure 3.2 Photograph of functionalization process set up

3.2.2 Functionalization of CNT with Polyethylene glycol

Portion of the oxidized CNT were further functionalized with polyethylene glycol. This is because the oxidized CNT has sites which enable for modification of the CNT surface [38].

In 250 ml flask, polyethylene glycol was melted on hotplate at 80°C, and then the oxidized CNT was added in a ratio of 1:10. The mixture stirred for 10 minutes. After that, a few drops of sulfuric acid as a catalyst were added. After addition of catalyst, the reaction kept on hotplate and stirred under reflux for 6 hours. Figure 3.3 gives the reaction mechanism for this step. After completion of the reaction, the mixture was poured in 250 ml of toluene and vacuum-filtered through a filter paper, the washing process was repeated for several times to remove any traces of un-reacted of PEG followed by washing with deionized water to remove any un-reacted sulfuric acid and then the produced CNT-PEG material dried in a vacuum oven at 80°C.

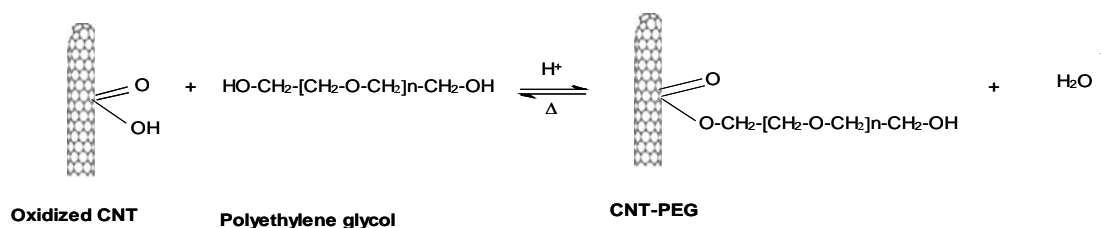


Figure 3.3 Chemical modification of oxidized CNT with PEG

3.2.3 Functionalization of CNT with Dodecylamine

Dodecylamine was heated until it melted and kept at a temperature of 40°C on a hot plate with stirrer. Then, oxidized CNT was added to the melted dodecylamine in a ratio 1: 10. The mixture was stirred continuously for 10 minutes. After that, a few drops of sulfuric acid were added to activate the reaction. The reaction was allowed to proceed under refluxing and constant agitation for 6 hours after which the mixture was washed with toluene to remove any un-reacted dodecylamine followed by washing with deionized water to remove excess acid. Subsequently, drying was carried out in a vacuum oven at 80°C. The resulting CNT is referred to as CNT-Amine. Figure 3.4 gives the reaction mechanism for this step.

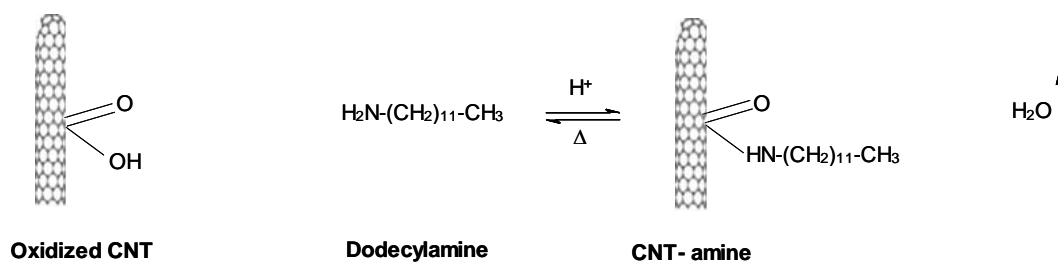


Figure 3.4 Chemical modification of oxidized CNT with dodecylamine

3.2.4 Functionalization of CNT with Octadecanol

In a 250 ml beaker, the octadecanol is melted on a hotplate at 90°C. Then, oxidized CNT was added to the melted octadecanol in a ratio 1: 10. The mixture was stirred continuously for 10 minutes before a few drops of sulfuric acid were added as a catalyst. After addition of the catalyst, the mixture was maintained on the hotplate and stirred for 6 hours. Upon completion of the reaction, the mixture was poured into 250 ml of toluene and vacuum-filtered through a filter paper. This washing operation was repeated several times to remove any un-reacted octadecanol and followed by washing with deionized water to remove excess acid. After that, the functionalized MMWCNT material produced was dried in a vacuum oven at 90°C. Figure 3.5 gives the reaction mechanism for this step.

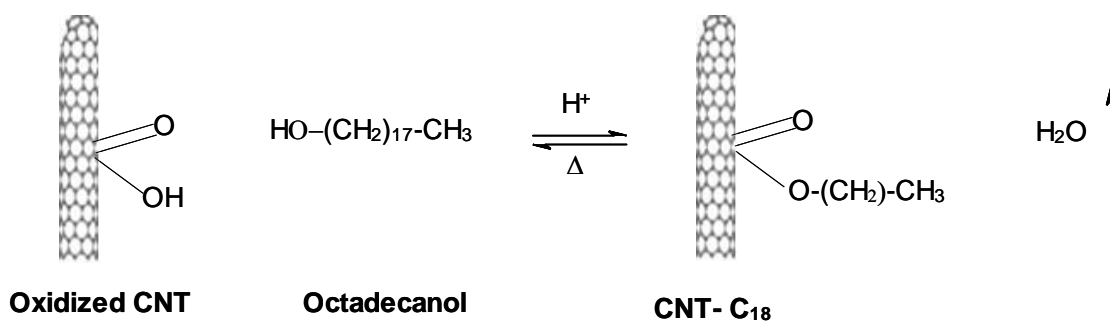


Figure 3.5 Chemical modification of oxidized CNT with octadecanol

3.2.5 Functionalization of CNT with Phenol

Phenol was heated until it melted and kept at a temperature of 45°C on a hot plate with stirrer. Then, oxidized CNT was added to the melted phenol in a ratio 1: 10.

The mixture was stirred continuously for 10 minutes. Then, a few drops of sulfuric acid were added as catalyst. The reaction was allowed to proceed under refluxing and constant agitation for 6 hours. After the completion of the reaction, the mixture was washed with toluene to remove any un-reacted phenol followed by washing with deionized water to remove excess acid. Then, drying was done in a vacuum oven at 80°C. The resulting CNT is referred to as CNT-Phenol. Figure 3.6 gives the reaction mechanism for this step.

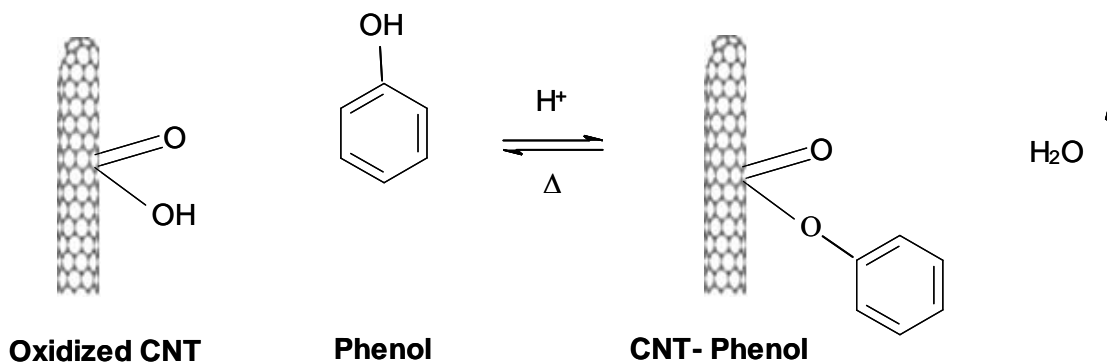


Figure 3.6 Chemical modification of oxidized CNT with phenol

3.3 Modification of CNT by Wet Impregnation Technique

The Impregnation is a famous method in the development of heterogeneous catalysts. The objective from using this technique in this study is to produce effective metallic nanoparticles with better metal macroscopic and microscopic distribution in carbon nanotubes.

Wet impregnation method was employed in the preparation of CuO-MWCNTs and Al₂O₃-MWCNTs. The impregnation procedure was carried out by using two aqueous solutions of cupric nitrate extra pure (trihydrate) Cu(NO₃)₂.3H₂O and aluminum nitrate Al(NO₃)₃.9H₂O. The reaction then followed by calcination under high temperature. Adsorption process, which occurs during wet impregnation, helps metallic nanoparticles to be introduced into the CNT matrix. As a result of that, nanostructured composite materials formed by carbon nanotubes and metal oxide-nanoparticles have given promising stable nanofluids as discovered in this study.

3.3.1 Steps of Metal Oxide Impregnation into the CNT Matrix

In a 100 ml beaker, cupric nitrate is added to as-received MWCNT in a ratio 1: 10. Then, ethanol with amount that is enough to submerge all materials in the beaker was added. The reaction inside the beaker was under the effect of ultra-sonication with 40 % power intensity for 30 min. After that, the mixture was dried in a vacuum oven at 90°C to remove excess ethanol and grinded.

Then, the material was calcinated in a furnace in presence of excess amount of Ar under 380-400°C for 3 to 4 h in order to give better morphologic characteristics and disposition of the of CuO nanoparticles on the surface of CNTs by forming oxides surfaces. The same procedure then was repeated for aluminum nitrate impregnation.

Heat treatment at high temperature decomposed the nitrate salt solutions, forming oxide phase [39]. The loading of the oxides can be increased by repeating the impregnation process. The decomposition temperature of the impregnated metal salt solution at 400°C improve the deposition of very fine and nano-sized oxide phases in the impregnated metal oxide to give the unique advantages of the wet impregnation method in the development of metal oxide-MWCNT with a fine microstructure [40].

3.4 Characterization

The functionalized MWCNTs obtained using different functional groups and prepared using the esterification reaction were analyzed using Fourier Transform Infrared Spectroscopy (FTIR) and thermal analysis, especially Thermo-Gravimetric Analysis (TGA) and Differential Scanning Calorimetry (DSC), while impregnation of carbon nanotubes with copper oxide (CuO) and aluminum oxide (Al₂O₃) were characterized by Scanning Electron Microscopy (SEM) and Energy Dispersive X-ray analysis (EDX).

3.4.1 Fourier Transform Infrared Spectroscopy (FTIR)

Fourier Transform Infrared Spectroscopy (FTIR) is a powerful tool for identifying types of chemical bonds (functional groups) in a molecule by producing an infrared absorption spectrum that is like a molecular "fingerprint". FTIR is most useful for identifying chemicals that are either organic or inorganic. It can be utilized to determine the quantity of some components of an unknown mixture. It can be applied to the analysis of solids, liquids and gasses. The term Fourier Transform Infrared Spectroscopy (FTIR) refers to a fairly recent development in the manner in which the data is collected and converted from an interference pattern to a spectrum. Today's FTIR instruments are computerized which makes them faster and more sensitive than the older dispersive instruments [41].

This technique works on the fact that bonds and groups of bonds vibrate at characteristic frequencies. A molecule which is exposed to infrared rays absorbs infrared energy at frequencies which are characteristic to that molecule. During FTIR analysis, a spot on the specimen is subjected to a modulated IR beam. The specimen's transmittance and

reflectance of the infrared rays at different frequencies is translated into an IR absorption plot consisting of reverse peaks. The resulting FTIR spectral pattern is then analyzed and matched with known signatures of identified materials in the FTIR library. However, (FTIR) Spectroscopy has shown limited ability to probe the structure of MWCNTs. A factor that has hindered the advancement of FTIR as a tool for MWCNTs analysis is the poor infrared transmittance of MWCNTs due to their black character [42]. A solution to this was the use of KBr preparations of carbon nanotube samples.

3.4.1.1 Samples Preparation

FTIR samples were prepared by grinding a very low concentration of dry material with potassium bromide (KBr) to form a very fine powder. This powder is then compressed into a thin pellet which can be analyzed. As indicated above, this very low concentration of MWCNTs is necessary due to the strong absorption characteristic of the nanotubes. In this study the spectra of the analyzed samples were recorded by Nicolet 6700 FTIR Spectrometer as shown in Figure 3.7.



Figure 3.7 Photograph of Nicolet 6700 FTIR Spectrometer

3.4.2 Thermal Analysis

Thermo-Gravimetric Analysis (TGA) measures changes in weight of a sample with increasing temperature. Moisture content and the presence of volatile species can be determined with this technique. Computer-based methods can be used to calculate weight percent losses.

The Dynamic Thermo-Gravimetric (DSC) experiments were conducted using a Netzsch model STA 449 F3 Jupiter® simultaneous thermal analyzer (shown in Figure 3.8), allowing measurement of mass change and associated phase transformation energetic. The system employed for this work was equipped with a PtRh furnace capable of operation from 25 to 1500°C, the temperature being measured using type S thermocouple. The system is vacuum tight, allowing measurements to be carried out under controlled atmosphere. In these experiments, Differential Scanning Calorimetry (DSC) measurements were also recorded to study phase transitions and exothermic/endothermic decompositions taking place in the samples investigated [37].

3.4.2.1 Samples Preparation

TGA-DSC analysis was performed on small samples (about 6 mg), mounted on platinum crucibles with Al₂O₃ liners and pierced lids, in an inert Ar atmosphere (flow rate of argon gas, 70 ml/min). The temperature range was varied from room temperature to 1400°C and the typical heating rate was 20°C/min, while the digital resolution of the balance was 1 µg/digit.



Figure 3.8 Photograph of Netzsch model STA 449 F3 Jupiter® devise

3.4.3 Scanning Electron Microscopy (SEM)

The scanning electron microscopy (SEM JEOL 5800 LV) equipped with an energy dispersive X-ray (EDX) analysis system was used to characterize the morphology and the elemental composition of impregnated carbon nanotubes with copper oxide (CuO) and aluminum oxide (AL₂O₃).

Scanning electron microscopy is utilized for inspecting topographies of specimens at very high magnifications using a piece of equipment called the scanning electron microscope. During SEM inspection, a beam of electrons is focused on a spot volume of the specimen, resulting in the transfer of energy to the spot. These bombarding electrons, also referred to as primary electrons, dislodge electrons from the specimen itself. The dislodged electrons, also known as secondary electrons, are attracted and collected by a positively biased grid or detector, and then translated into a signal [43].

To produce the SEM image, the electron beam is swept across the area being inspected, producing many such signals. These signals are then amplified, analyzed, and translated into images of the topography being inspected. Finally, the image is shown on a CRT. The energy of the primary electrons determines the quantity of secondary electrons collected during inspection. The emission of secondary electrons from the specimen increases as the energy of the primary electron beam increases, until a certain limit is reached. Beyond this limit, the collected secondary electrons diminish as the energy of the primary beam is increased, because the primary beam is already activating electrons deep below the surface of the specimen. Electrons coming from such depths usually recombine before reaching the surface for emission [43].

Aside from secondary electrons, the primary electron beam results in the emission of backscattered (or reflected) electrons from the specimen. Backscattered electrons possess more energy than secondary electrons, and have a definite direction. As such, they cannot be collected by a secondary electron detector, unless the detector is directly in their path of travel. All emissions above 50 eV are considered to be backscattered electrons. Backscattered electron imaging is useful in distinguishing one material from another, since the yield of the collected backscattered electrons increases monotonically with the specimen's atomic number. Backscatter imaging can distinguish elements with atomic number differences of at least 3, i.e., materials with atomic number differences of at least 3 would appear with good contrast on the image [43].

A SEM may be equipped with an EDX analysis system to enable it to perform compositional analysis on specimens. EDX analysis is useful in identifying materials and contaminants, as well as estimating their relative concentrations on the surface of the specimen. EDX Analysis stands for Energy Dispersive X-ray analysis. It is sometimes referred to also as EDS or EDAX analysis. It is a technique used for identifying the elemental composition of the specimen, or an area of interest thereof. The EDX analysis system works as an integrated feature of a scanning electron microscope (SEM), and cannot operate on its own without the latter [43].

During EDX Analysis, the specimen is bombarded with an electron beam inside the scanning electron microscope. The bombarding electrons collide with the specimen atoms' own electrons, knocking some of them off in the process. A position vacated by an ejected inner shell electron is eventually occupied by a higher-energy electron from an

outer shell. To be able to do so, however, the transferring outer electron must give up some of its energy by emitting an X-ray [43].

The amount of energy released by the transferring electron depends on which shell it is transferring from, as well as which shell it is transferring to. Furthermore, the atom of every element releases X-rays with unique amounts of energy during the transferring process. Thus, by measuring the amounts of energy present in the X-rays being released by a specimen during electron beam bombardment, the identity of the atom from which the X-ray was emitted can be established [43]. Figure 3.9 shows the photograph of SEM JEOL 5800 LV.



Figure 3.9 Photograph of SEM JEOL 5800 LV Unit

3.5 Preparation of Nanofluids

The two-step method which is a process by dispersing nanoparticles into base liquids was used for preparing nanofluids. Deionized water with functionalized and impregnated MWCNTs was used to produce nanofluids. In case of functionalized MWCNT, nanofluid was prepared by adding the calculated amount of functionalized MWCNT in a known amount of deionized water base fluid in a beaker and sonicated for 30 min .The ultrasonic pulses of 750 W and 20 kHz generated by an ultrasonic cell disrupter (shown in Figure 3.10) were used to improve the dispersion of MWCNT into the base fluid. In case of impregnated MWCNT, sodium dodecyl sulfate (SDS) was used as a dispersing agent.



Figure 3.10 Photograph of an ultrasonic cell disrupter

3.6 Measurement of Thermal Conductivity

The thermal conductivity measurement of nanofluid was achieved using the modified transient plane source technique. In this work, the Mathis TCi system which is shown in Figure 3.11 was used in to measure the thermal conductivity.



Figure 3.11 The Mathis TCi Thermal Conductivity Analyzer

This device is based on the modified transient plane source technique. It uses a one-sided, interfacial, heat reflectance sensor that applies a temporary, constant heat source to the sample. The difference between this method and traditional hot wire techniques is that the heating element is supported on a backing, which provides mechanical support, electrical insulation and thermal insulation. This modification eliminates the intrusive nature of the hot wire method and provides the capability to test smaller volumes of material as the wire is coiled as shown in Figure 3.12[44].

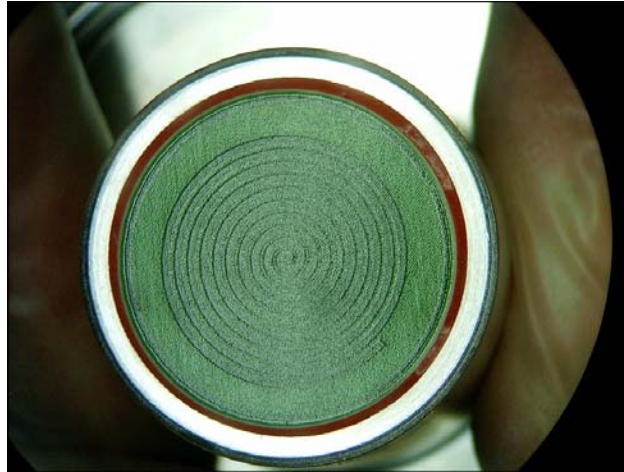


Figure 3.12 Sensor face –diameter is 17 mm.

The test is achieved by pouring 30 ml of the sample liquid into a 50 ml Pyrex beaker. Then, the sensor with heating element is placed into the beaker for a resident amount of time of typically 1 to 3 seconds. A known current is applied to the sensor's heating element providing a small amount of heat. The heat provided results in a rise in temperature at the interface between the sensor and the sample – typically less than 2 °C. This temperature rise at the interface causes a change in the voltage drop of the sensor element.

Since the rate of temperature rise at the heating element is inversely proportional to the thermal conductivity of the material, this property of material can be determined by measuring the rate of voltage rise when a constant current is utilized. Voltage increase can be correlated with thermal conductivity through a calibration with reference materials having known thermal conductivity. From this calibration, the thermal conductivity of unknown materials can be measured [44].

3.7 Experimental Setup and Calculations

To investigate the performance of nanofluid in a heat exchanger, an experimental apparatus was designed and constructed as shown schematically in Figure 3.13. The experimental set up mainly consists of a concentric tube heat exchanger. The test section consisted of 1.59 m annular tube which was constructed of 13.5 mm diameter inner copper tube with 1.25 mm thickness and 22.5 mm diameter outer glass tube. In order to minimize the heat loss, the hot fluid (nanofluid) flows in the inner tube, while the cold fluid in outer tube.

Two water bathes are provided to keep the fluid circuits at constant temperature. Four thermocouples (K-type) are available to measure the inlet and outlet temperatures. Using four selector switches easily makes the temperature readings from those thermocouples. The flow rates of hot and cold fluids are measured using rotameters, connected to the inner and outer tubes. The flow is controlled with two globe valves, one at nanofluid loop and the other at cooling fluid loop.

Nanofluid, with different particle weight percentages, was used to determine the effect of the nanoparticle concentration on effectiveness of heat exchanger, the percentages being 0.05%, 0.1% and 0.2%.

During experimental runs, the inlet and outlet temperatures of the streams and volume flow rates are measured at steady state conditions. From these data, the effectiveness can be determined from the following relations [45]:

$$q = \dot{m}_h C_{p_h} (T_{h,in} - T_{h,out}) \quad (3-1)$$

$$q_{\max} = (\dot{m} C_p)_{\min} (T_{h,in} - T_{c,in}) \quad (3-2)$$

$$\varepsilon = \frac{q}{q_{\max}} \quad (3-3)$$

Where:

q : Heat transfer rate.

\dot{m} : Mass flow rate.

Cp : Specific heat capacity.

T : Temperature.

q_{\max} :The maximum possible heat transfer rate.

ε : The effectiveness of the heat exchanger.

h : Subscript for hot fluid.

c : Subscript for cold fluid

The thermal properties are calculated at the average temperatures of the inlet and outlet streams. Experiments were performed for volume flow rates ranging from 1 l/min to 2.6 l/min for nanofluid and 1.52 l/min for cooling water.

At a given flow rate, the *effectiveness enhancement* of using nanofluid can be calculated as follows

$$\varepsilon = \frac{\mathcal{E}_{\text{Nanofluid-water}} - \mathcal{E}_{\text{Water-Water}}}{\mathcal{E}_{\text{Water-Water}}} * 100 \quad (3-4)$$

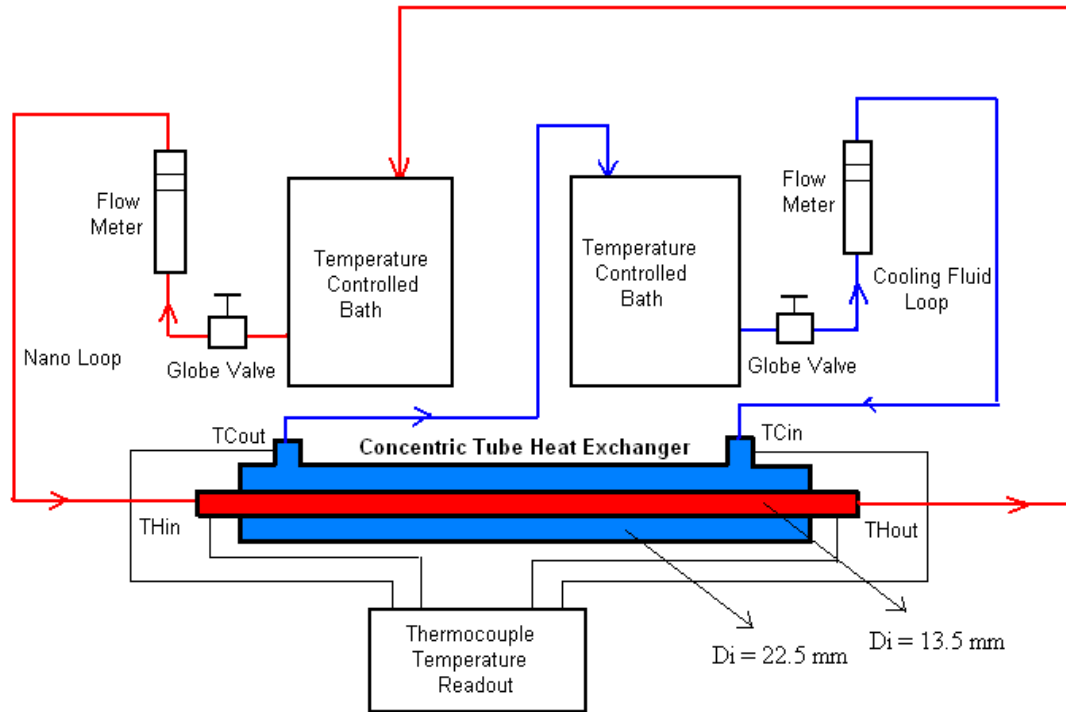


Figure 3.13 Schematic layout of the experimental set up



Figure 3.14 Photograph of the experimental set up

CHAPTER FOUR

4 RESULTS AND DISCUSSIONS

4.1 Characterization of Functionalized and Impregnated Carbon Nanotubes

This section presents and discusses the results of the characterization of functionalized carbon nanotubes using Fourier Transfer Infrared (FTIR) and Thermo-Gravimetric Analysis (TGA). This section also includes the results and discussion of the characterization of impregnated carbon nanotubes using Scanning Electron Microscopy (SEM) and Energy Dispersive X-ray analysis (EDX).

4.1.1 Characterization of Functionalized Carbon Nanotubes by FTIR

4.1.1.1 Acid Oxidized Carbon Nanotubes

The FTIR spectrum for the oxidized CNT is depicted in Figure 4.1. The peak appearing in the region 1737 cm^{-1} can be attributed to the presence of carbonyl group while those in the region of 3426 and 3728.71 cm^{-1} are due to the presence of hydroxyl groups [46,47,48,49,50]. The peak at 1560 cm^{-1} is related to the carboxylate anion stretch mode [51]. The peaks at around 2922 and 2853 cm^{-1} correspond to the H-C stretch of C-H=O

in carbonyl group. The existence of these peaks is an indication of the presence of oxygen containing groups which implies successful oxidation of the CNT surface.

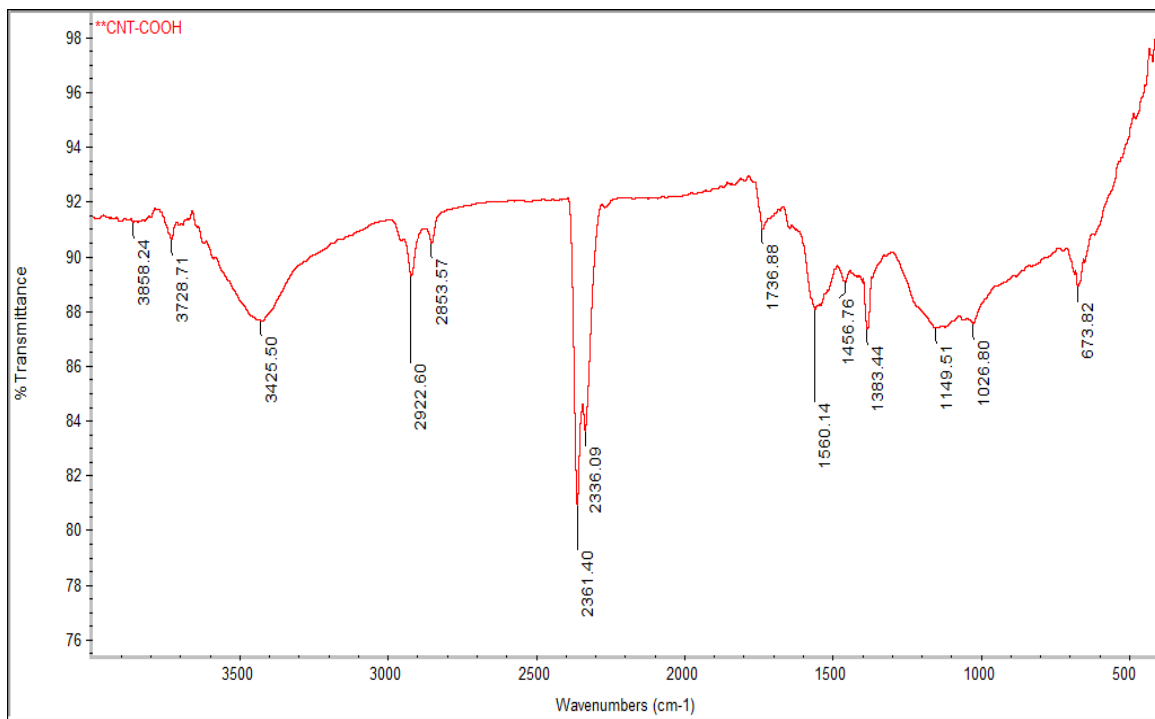


Figure 4.1 FTIR spectra of oxidized CNT

4.1.1.2 Carbon Nanotubes Functionalized with Polyethylene Glycol

The FT-IR spectrum in Figure 4.2 is that of CNT functionalized with polyethylene glycol (PEG). The peak at 2922 cm^{-1} can be attributed to symmetric and asymmetric C–H stretching of methylene group in polyethylene glycol. The new peak at wave length of 1084 cm^{-1} is due to the C–O stretch of ester. Increased strength of the signal at 3428 cm^{-1} may be associated with O–H stretching vibration of the hydroxyl group in PEG.

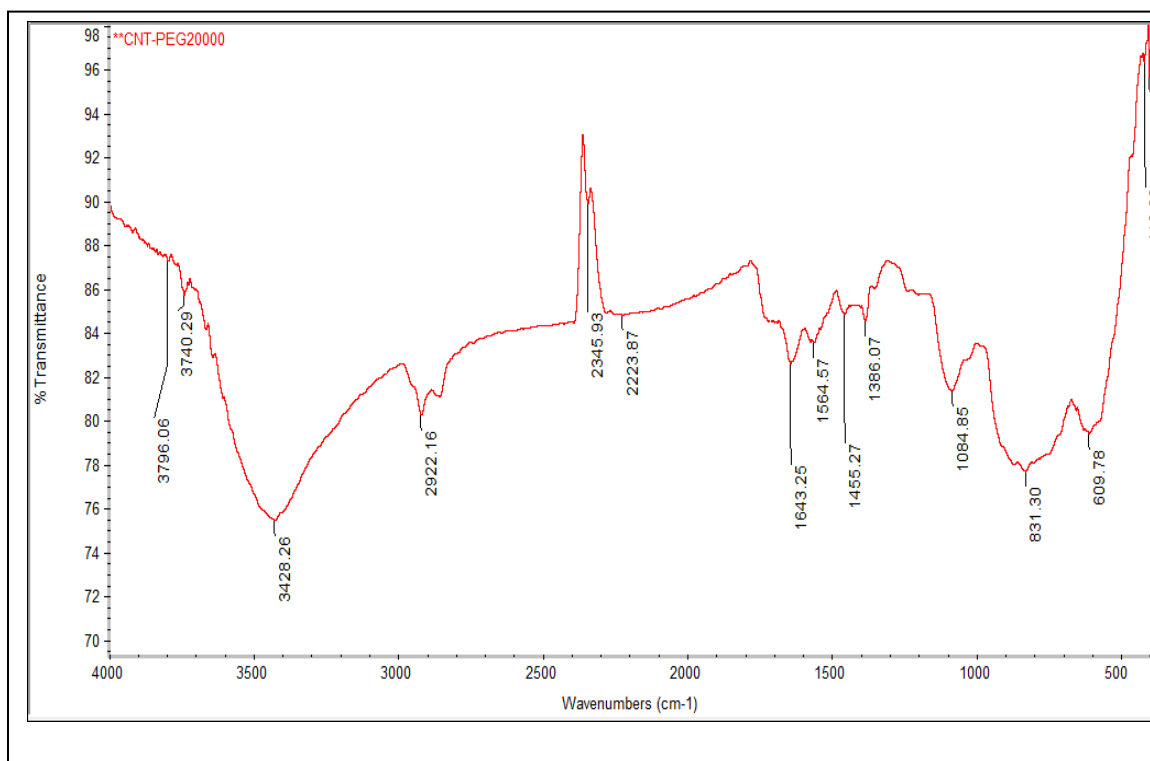


Figure 4.2 FTIR spectra of CNT functionalized with polyethylene glycol

4.1.1.3 Carbon Nanotubes Functionalized with Dodecylamine

The spectrum in Figure 4.3 is that of CNT functionalized with dodecylamine. There is a new large peak existing at wave length region of 1115 cm^{-1} which is indication of C–N stretching band of amine compound used for functionalized process which is absent in Figure 4.1. The peak at 1575 cm^{-1} is due to N–H bending of amide. The peaks at 2920 and 2851 cm^{-1} are due to C–H stretching vibrations: asymmetric and symmetric modes of methylene groups of dodecylamine which is confirmation of the presence of dodecylamine on the CNT surface.

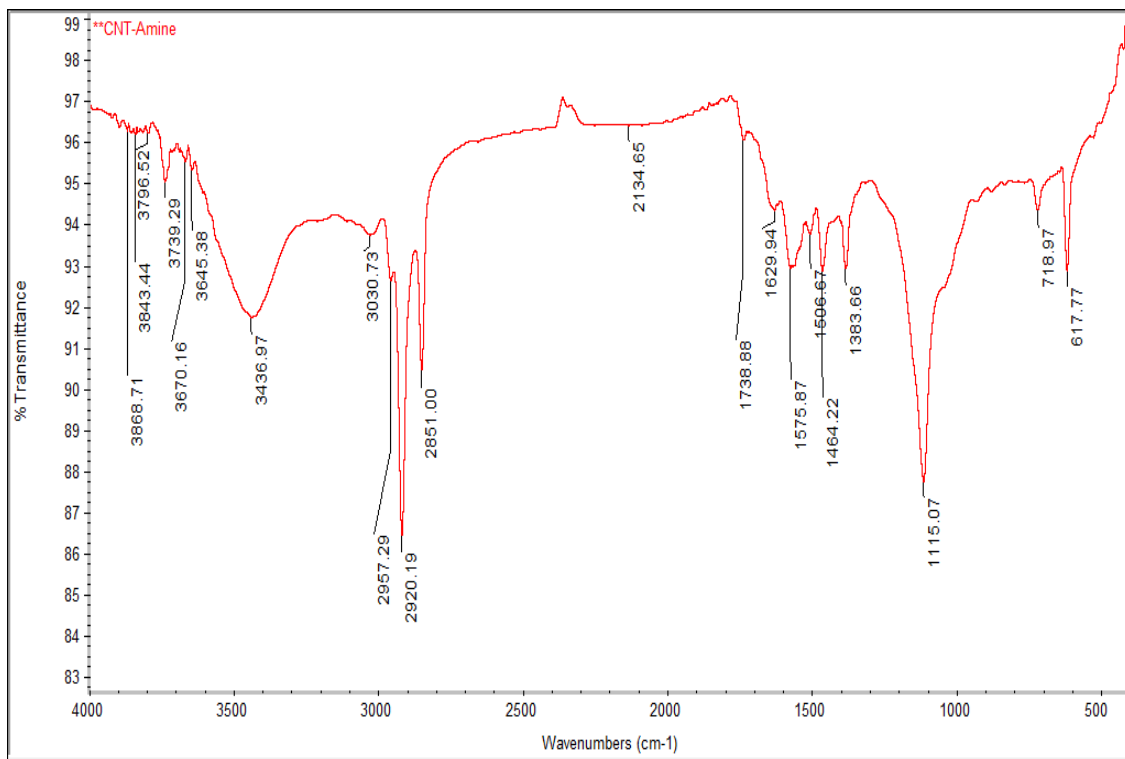


Figure 4.3 FTIR spectra of CNT functionalized with dodecylamine

4.1.1.4 Carbon Nanotubes Functionalized with Phenol

Figure 4.4 shows the spectrum of CNT functionalized with phenol. The peak at wave length 1564 cm^{-1} is due to the C=C asymmetric stretch of aromatic rings of phenol. The large peak existing at wave length region of 1135 cm^{-1} is characteristic of C–O stretch of ester group. The new peaks at appearing at wave length 829 cm^{-1} , 751 cm^{-1} and 646 cm^{-1} correspond to C–H 'oop' bend from the aromatic ring of the phenol.

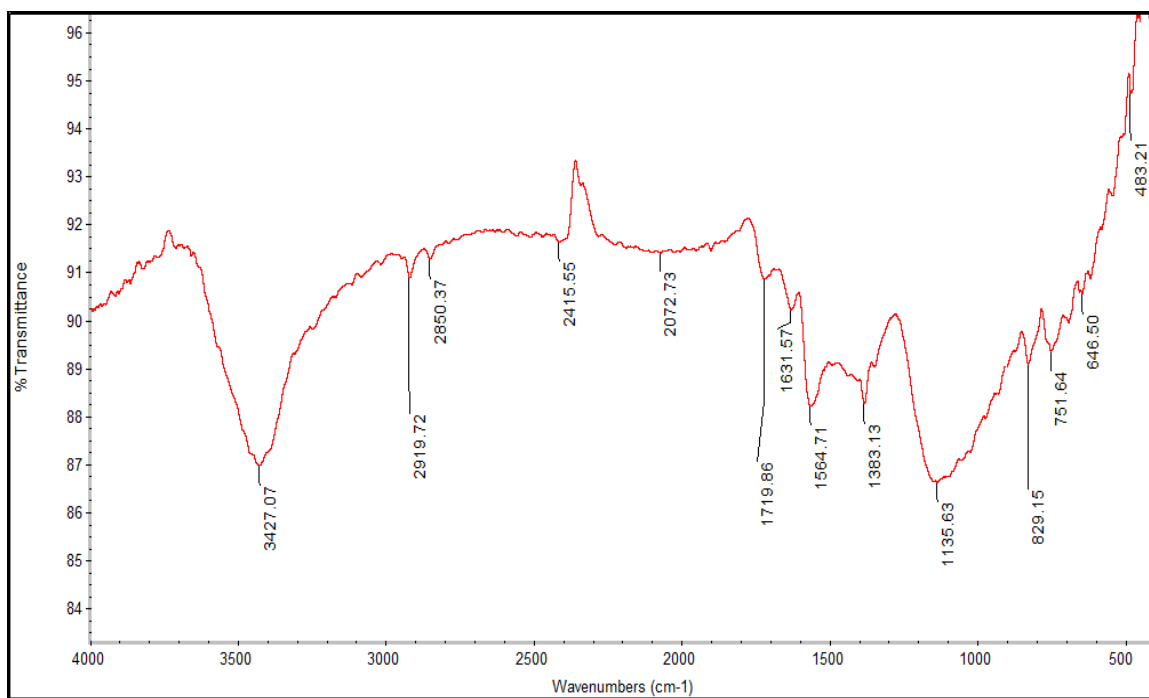


Figure 4.4 FTIR spectra of CNT functionalized with phenol

4.1.1.5 Carbon Nanotubes Functionalized with Octadecanol

The spectrum in Figure 4.5 is that of CNT functionalized with octadecanol. The large peak existing at wave length region of 1122 cm^{-1} is characteristic of C–O stretch of ester group. The peaks at 2929 and 2850 cm^{-1} are due to C–H stretch modes, which is indicative of the presence of a long-chain alkyl molecule (octadecanol).

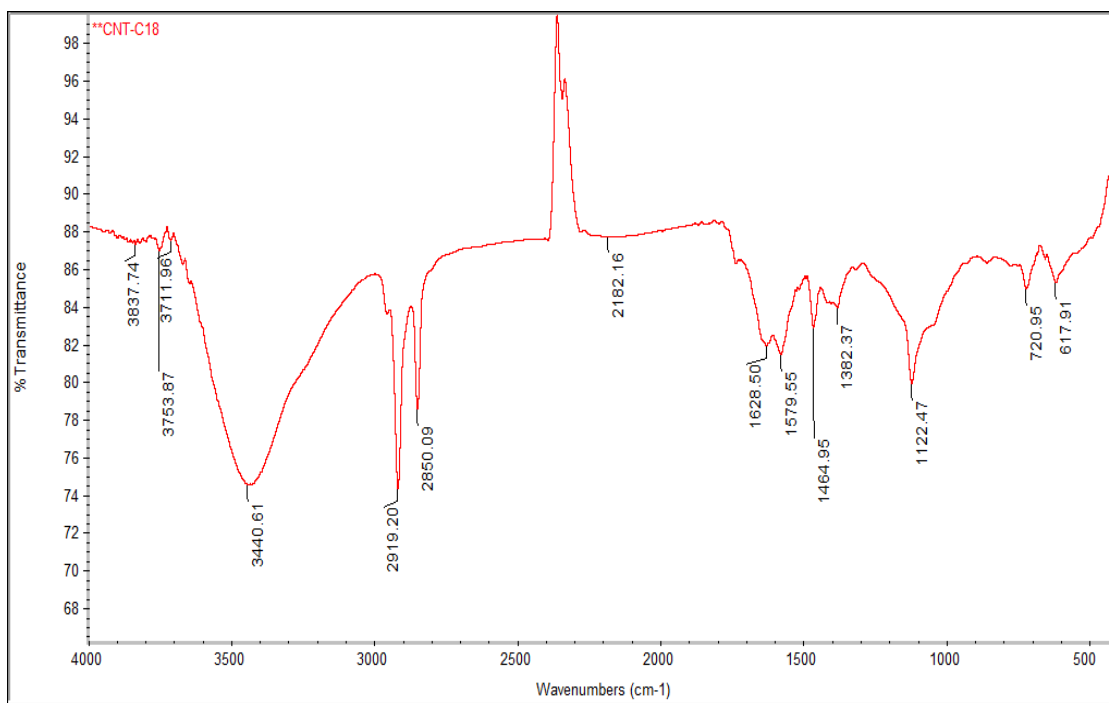


Figure 4.5 FTIR spectra of CNT functionalized with octadecanol

4.1.2 Thermal Degradation Analysis of Functionalized Carbon

Nanotubes

The study of the thermal degradation of materials is of major importance since it can, in many cases; determine the upper temperature limit of use for a material. In addition, considerable attention has been directed towards the exploitation of thermo-gravimetric data for the determination of functional groups. For this purpose, Thermo-Gravimetric Analysis (TGA) is a technique widely used because of its simplicity and the information afforded by a simple thermogram [37].

Figures 4.6 through 4.10 Exhibit the TGA-DSC measurements for the carbon nanotubes functionalized with five different organic groups, namely CNT-COOH, CNT-PEG, CNT-Amine, CNT-Octadecanoate, and CNT-Phenol. In these figures, TG% stands for the temperature-dependent mass change in percent, DTG (% min) to the rate of mass change (the derivative of the TG curve), and DSC (mW/mg) to the heat flow rate into or out of the sample.

Several mass loss steps were observed below $\sim 150^{\circ}\text{C}$ which are due to the release of moisture and the decomposition of the associated organic groups. The mass loss steps were supported by endothermic peaks visible in the DSC signal, except for the sample CNT-COOH which exhibits one exothermic peak (Figure 4.6). As revealed by the DTG curve, the initial degradation of-COOH starts at approximately 170°C and reaches a maximum weight loss of this acidic group at about 321°C and completes at about 480°C . The second peak appearing at about 783°C corresponds to the oxidation of CNT due to the decomposition of the carboxylic group releasing oxygen into the chamber of the TGA-DSC system [37].

Figure 4.7 depicted the TGA–DSC curves for CNT-PEG, the two peaks at 260°C and 348°C in DTG curve assign to maximum degradation of poly ethylene glycol ester group and carboxylic acid group respectively. As shown in Figure 4.8, for the CNT–Amine, the two initial peaks, located at 287°C and 387°C, in the DTG curve correspond to the maximum degradation of the amine group (dodecylamide) and carboxylic acid group, respectively. Figure 4.9 displays the degradation of CNFOctadecanoate . Two peaks appear at 265°C and approximately 400°C, corresponding to the maximum degradation of the octadecanoate group and carboxylic acid group, respectively. It seems from Figure 4.10 that a small amount of phenol has been attached to the nanotubes through the carboxyl group, therefore yielding a small DTG peak appearing at about 250°C, corresponding to maximum degradation of phenol group, followed by a peak at 376°C showing the maximum degradation of the carboxylic acid group [37].

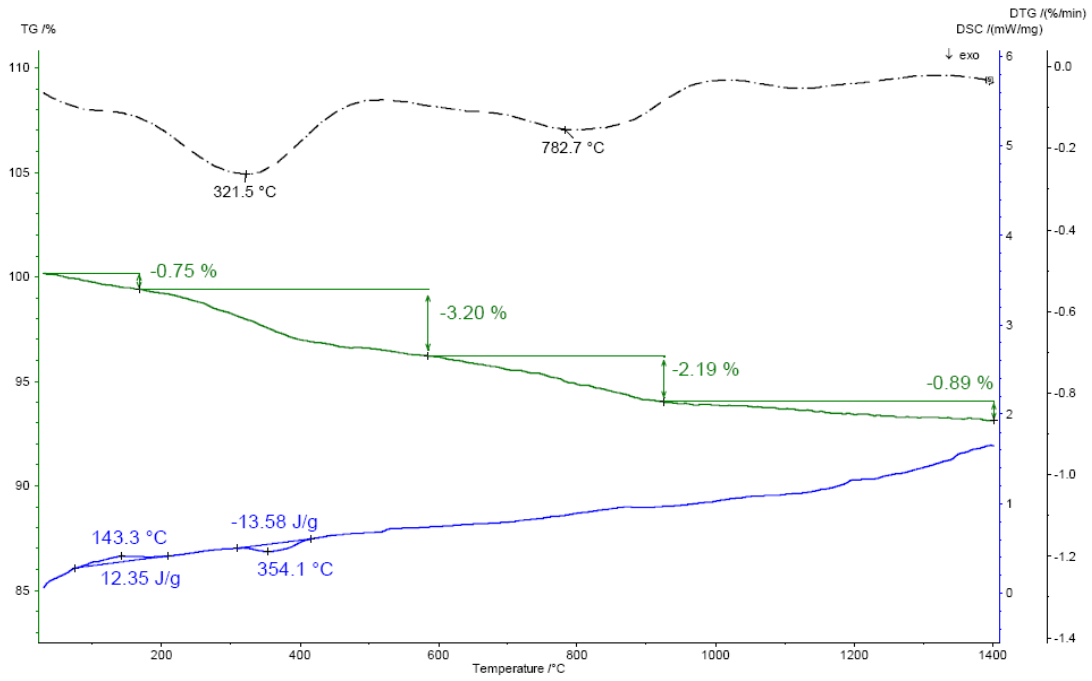


Figure 4.6 TGA-DSC curves for modified carbon nanotubes with carboxylic group

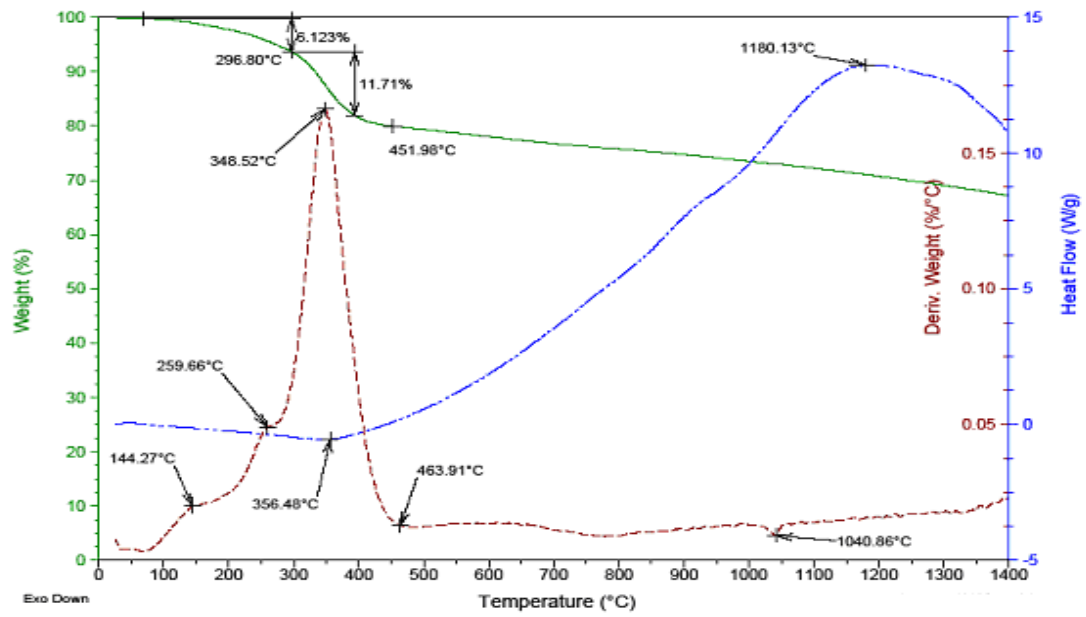


Figure 4.7 TGA-DSC curves for modified carbon nanotubes with poly ethylene glycol group

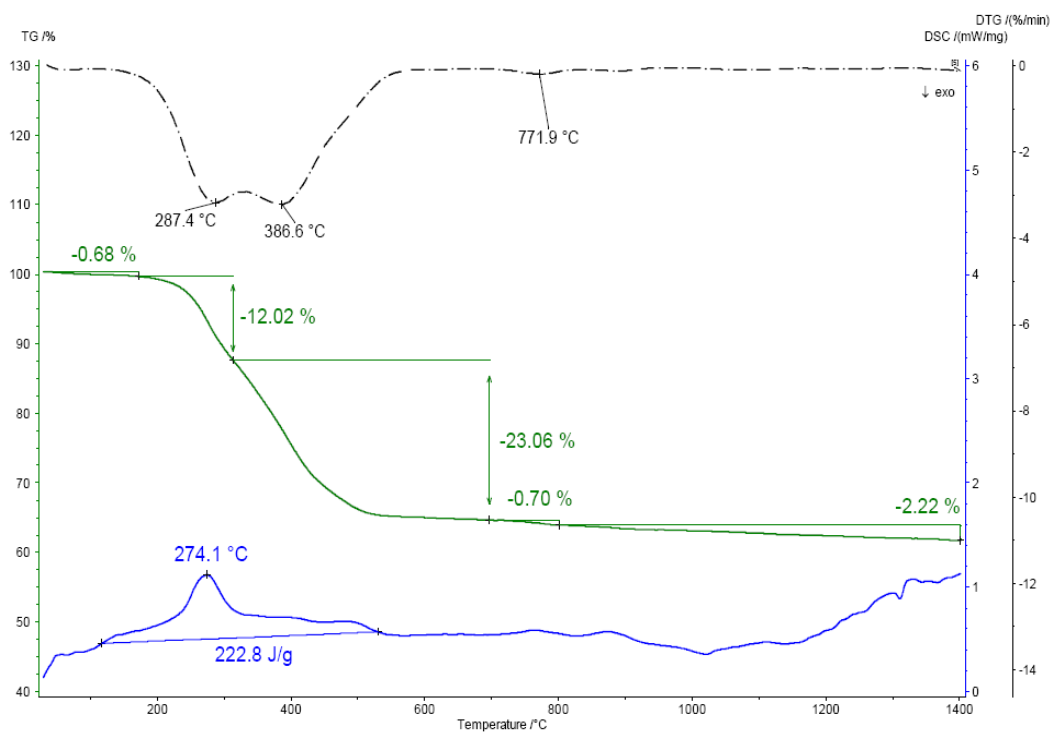


Figure 4.8 TGA-DSC curves for modified carbon nanotubes with amine group

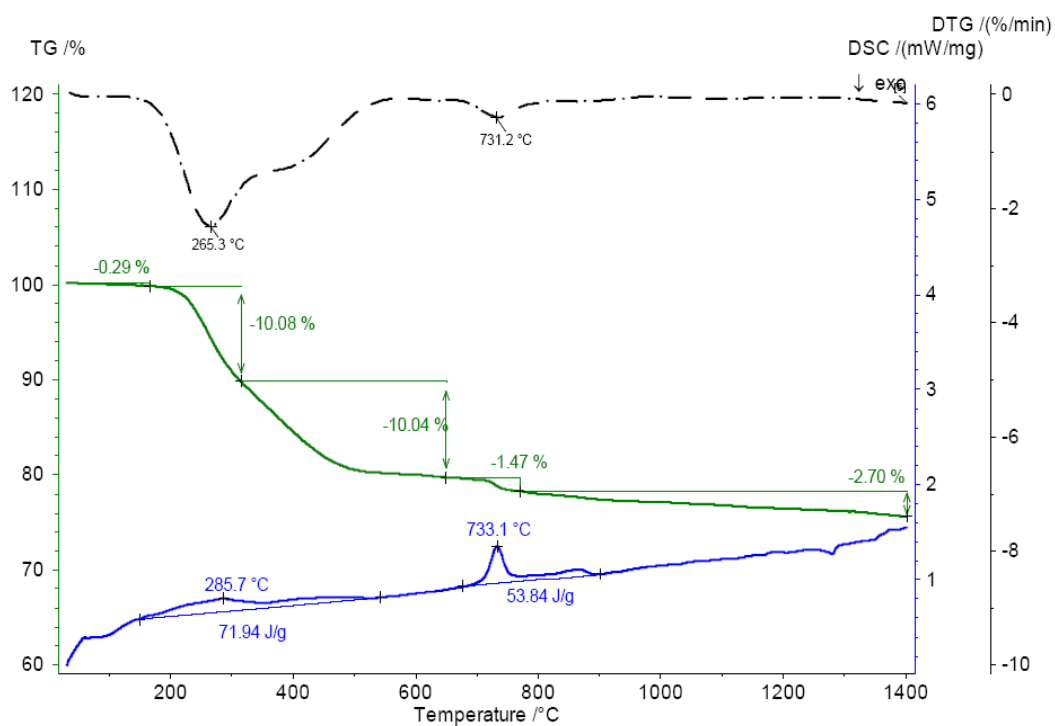


Figure 4.9 TGA-DSC curves for modified carbon nanotubes with octadecanoate group

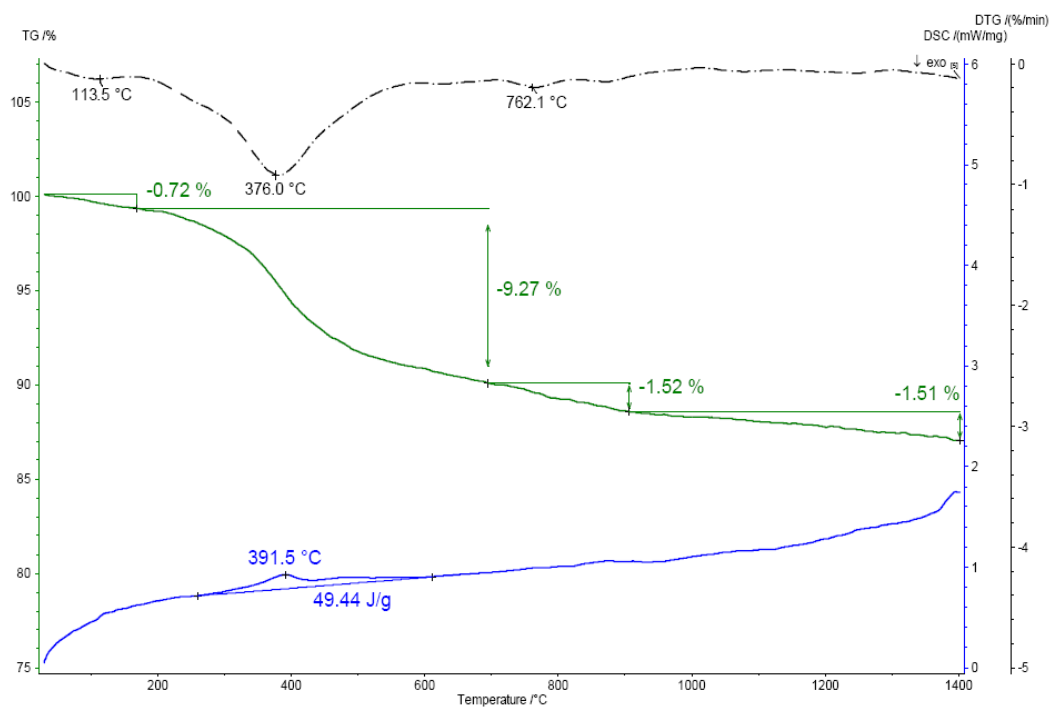


Figure 4.10 TGA-DSC curves for modified carbon nanotubes with phenol group

4.2 Characterization of Impregnated Carbon Nanotubes

4.2.1 Scanning Electron Microscopy Images

The morphologies of impregnated carbon nanotubes with metal oxides (copper oxide (CuO) and aluminum oxide (AL₂O₃)) were investigated by using scanning electron microscopy images (Model: SEM JEOL 5800LV). The imaging was conducted at varying magnifications in a secondary electron mode utilizing an accelerating voltage of 5.00keV. The chemical composition of samples was obtained using an energy dispersive X-ray spectrometer, equipped with SEM, fitted with an ultra –thin Be window. The samples were coated with conductive aluminum tape to increase the electrical conductivity before sent to vacuum chamber of SEM for EDX measurement.

Typical SEM micrographs, shown in Figure 4.11 and Figure 4.12 confirm formation of metal oxide on the surface of CNT and also exhibit the dispersion of doped element varies from position to other. The SEM images also show that, the impregnated carbon nanotubs with metal oxides were agglomerated to form large particles. High agglomeration can be attributed to lattice distortion of crystalline structure of carbon nanotubes.

4.2.2 Energy Dispersive X-ray Analysis

The existence of CuO and AL₂O₃ nanoparticles and their loading have been confirmed using Energy Dispersive X-ray analysis EDX. Figure 4.13 and Figure 4.14 show the energy dispersive spectroscopy (EDS) patterns of CuO and AL₂O₃ particles receptively. Combing with the scanning electron microscope, EDS is used to determine the chemical composition of a microscopic area of a solid sample. The two strong peaks in Figure 4.13

assign to Cu element, while the strong peak in Figure 4.14 corresponds to AL element. This indicates that, CuO and Al_2O_3 nanoparticles are successfully synthesized on the surface of carbon nanotubes using a wet impregnation method.

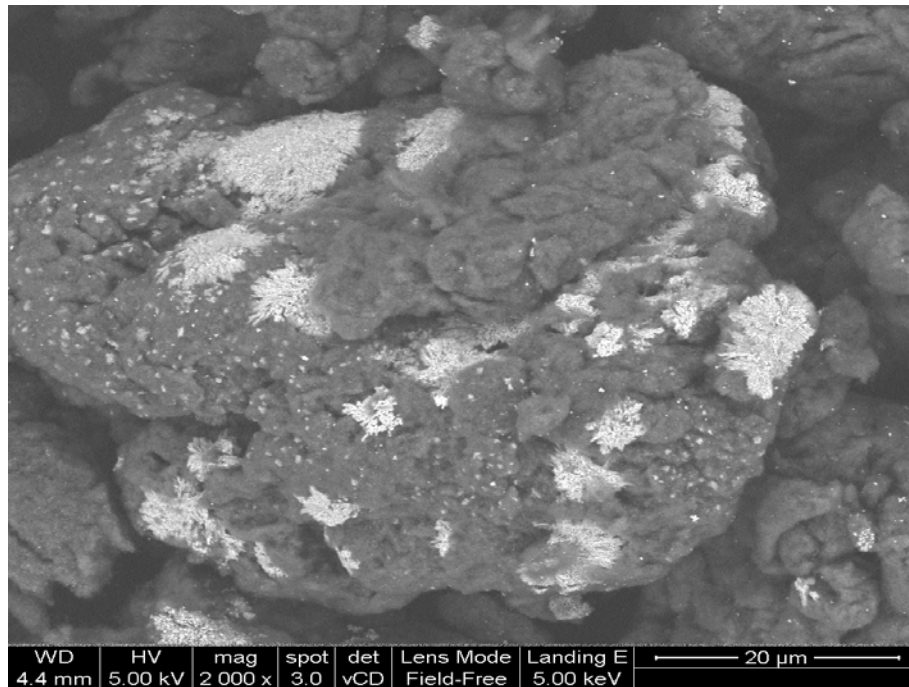


Figure 4.11 SEM image of MWCNTs-CuO

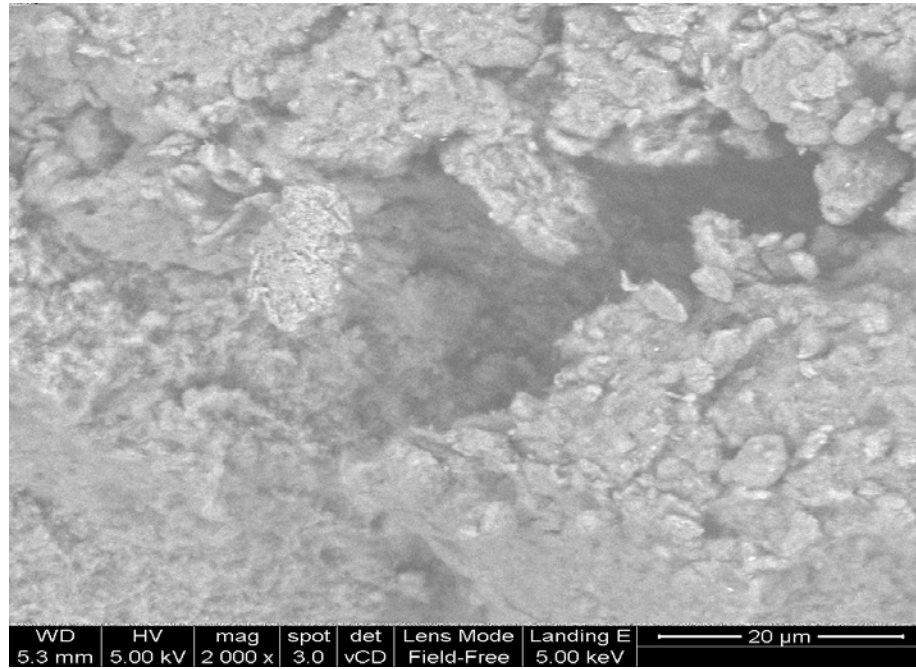


Figure 4.12 SEM image of MWCNTs-AL₂O₃

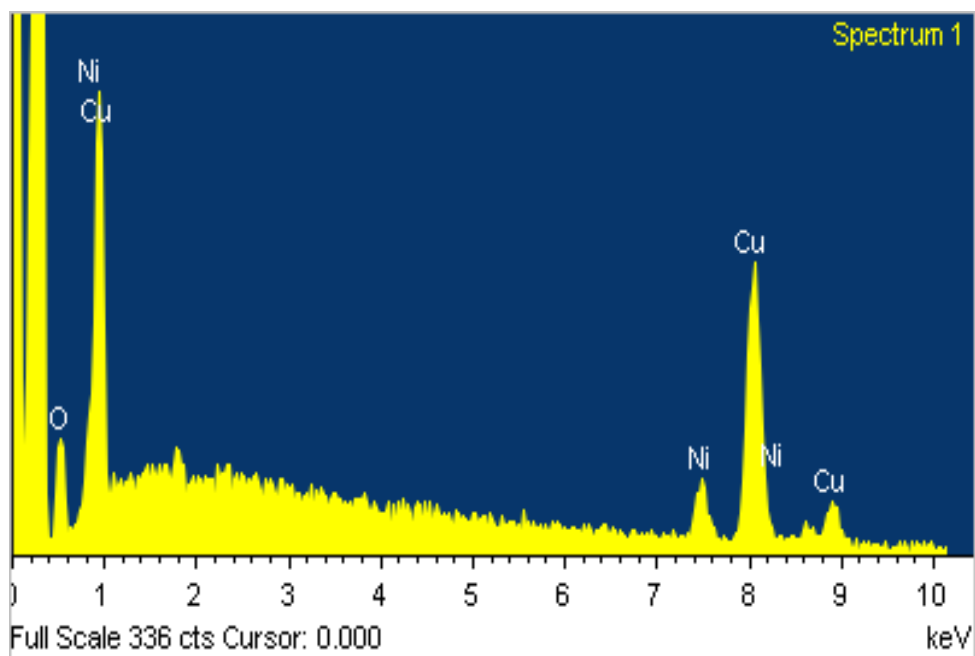


Figure 4.13 EDX pattern of MWCNTs-CuO

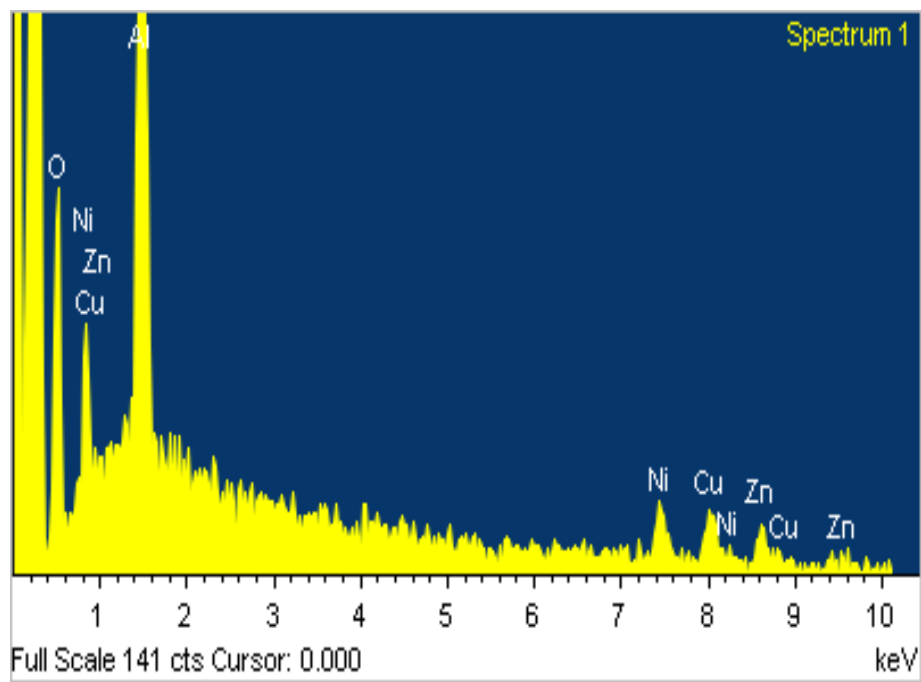


Figure 4.14 EDX pattern of MWCNTs-AL₂O₃

4.3 Stability Study

Nanofluids are a complicated mixture of liquid and solid particles. Nanoparticles tend to aggregate and participate with the time because of its high surface-activity. The agglomeration of nanoparticles causes not only the settlement and clogging of microchannels but also the decreasing of thermal conductivity of nanofluids. So the investigation on stability is also a key issue that influenced the properties of nanofluids for application. In this work, precipitation photograph of nanofluids in test tubes taken by a camera was used for observing the stability of nanofluids.

It is recognized that CNTs have a hydrophobic surface, which is prone to aggregation and precipitation in water in the absence of a dispersant [52]. Lots of efforts have been done in this stage of the work, searching for an appropriate material (functionalized CNT). After many trial and error tests, It was found that, oxidized CNT and CNT-PEG were able to prepare a stable nanofluid with water for more than two months without visually observable precipitation, while CNT-Amine nanofluid settled as shown in Figure 4.15. Functionalized carbon nanotubes with octadecanol and phenol failed to produce stable and homogeneous suspension with deionized water.

These findings can be attributed to the difference in the electronegativities of the atoms. It is clear that, the oxygen atom in H–O bond in oxidized CNT and CNT-PEG has greater electronegativity than the nitrogen atom in H–N bond in CNT-Amine. Therefore, the oxidized CNT and CNT-PEG will be more polarity than CNT-Amine and they can be easily dissolved into water, polar solvent, and make more stable and homogenous solutions.



Figure 4.15 Photographs of oxidized MWCNT and MWCNT-PEG nanofluid show no precipitation after two months

Impregnated carbon nanotubes with copper oxide (CuO) and aluminum oxide (Al₂O₃) were allowed to prepare stable and homogenous nanofluids with water in presence of sodium dodecyl sulfate (SDS) as a dispersing agent shown in Figure 4.16.



Figure 4.16 Photographs of impregnated MWCNT nanofluid show no precipitation in presence of SDS surfactant after two months

4.4 Thermal Conductivity Measurements

4.4.1 Effect of Concentration on Thermal Conductivity at Different Temperatures

In this section, the thermal conductivity enhancements of nanofluids composed of deionized water base fluid and different modified MWCNT nanoparticles are investigated.

4.4.1.1 Effect of Concentration on Thermal Conductivity for DI water+CNT-COOH Nanofluid

Figure 4.17 Exhibits the thermal conductivity enhancement for deionized water and CNT-COOH nanofluid. The thermal conductivities of the present system have been measured at weight fractions of 0.05%, 0.1%, 0.3% and 0.5% for different temperatures. The temperatures controlled by using a thermostat water bath. From the experimental results, it is clearly shown that the thermal conductivity enhancement increased with increasing nanoparticles weight concentration. Also, it is found that, the thermal conductivity enhancement decreased with increasing temperature especially at high particles load. This reduction in the enhancement may be attributed to the agglomeration of particles. The maximum enhancement of thermal conductivity was 3.4% observed for a weight concentration of 0.5% at 35°C.

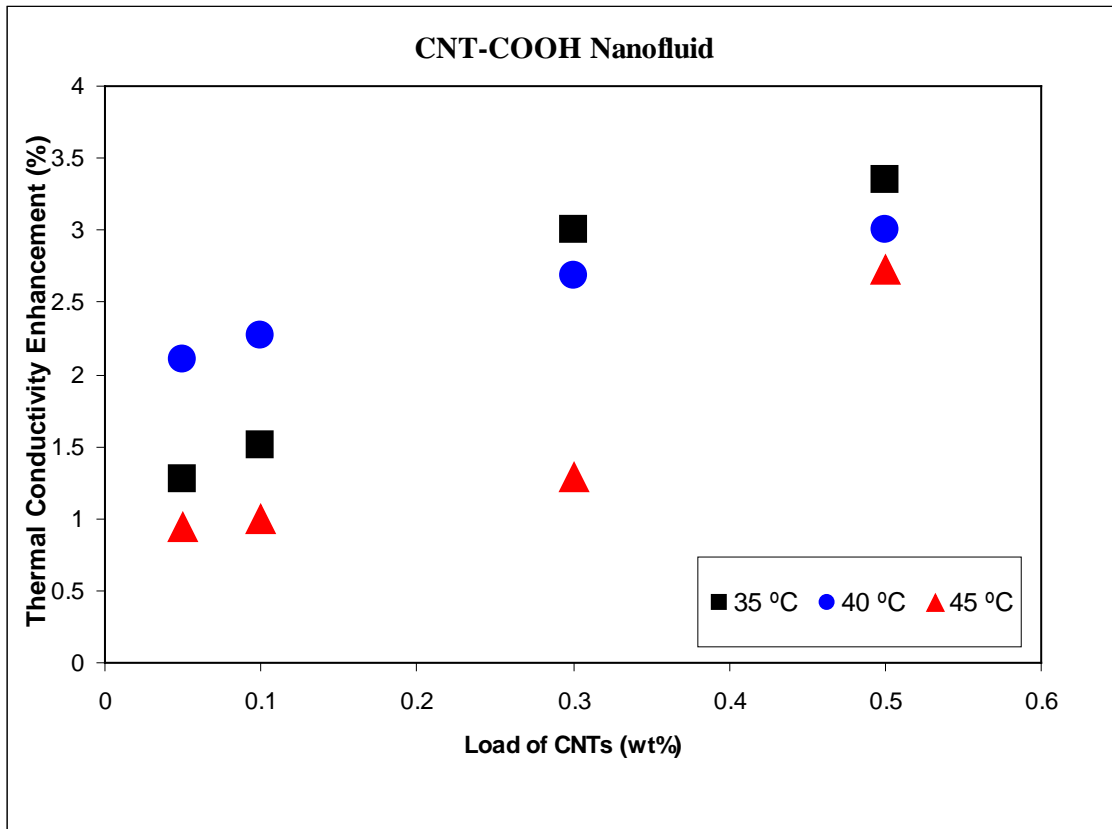


Figure 4.17 Thermal conductivity enhancement of DI water with CNT-COOH nanofluid

4.4.1.2 Effect of Concentration on Thermal Conductivity for DI water+CNT-PEG Nanofluid

Figure 4.18 shows the thermal conductivity enhancement for deionized water and CNT-PEG nanofluid. The thermal conductivities of the present system have been measured at weight fractions of 0.05%, 0.1%, 0.3% and 0.5% for different temperatures. From the experimental results, it is found that, the thermal conductivity enhancement increased with increasing nanoparticles load. Also, it is found that, the thermal conductivity enhancement decreased with increasing temperature particularly at high concentration of particles. The maximum enhancement of thermal conductivity was 4 % observed for a weight concentration of 0.5% at 35°C.

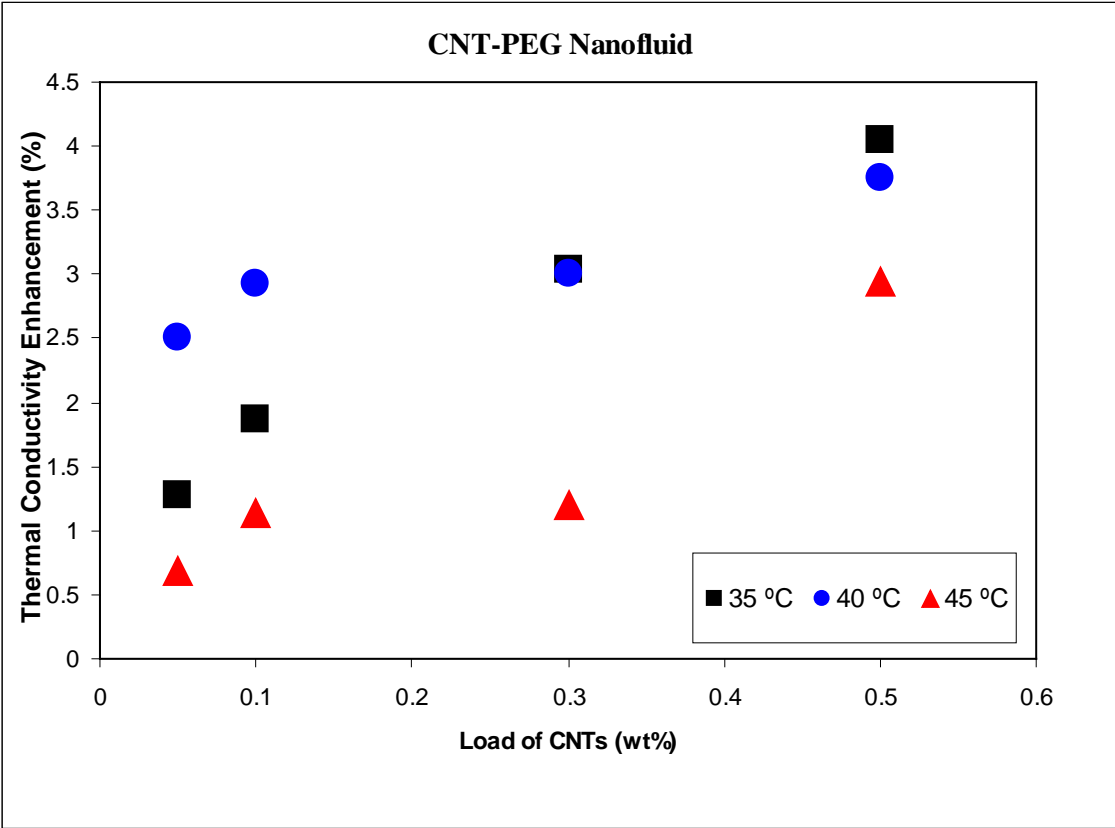


Figure 4.18 Thermal conductivity enhancement of DI water with CNT-PEG nanofluid

4.4.1.3 Effect of Concentration on Thermal Conductivity for DI water+CNT- AL₂O₃ Nanofluid

Figure 4.19 depicts the thermal conductivity enhancement for deionized water and CNT-AL₂O₃ nanofluid. The load of AL₂O₃ fixed at 10 wt % of CNT. The thermal conductivities of the present system have been measured at weight fractions of 0.05%, 0.1%, 0.3% and 0.5% for different temperatures. From the experimental results, it is clearly seen that, the thermal conductivity enhancement increased with increase in particles weight concentration for different temperatures. The enhancement decreased at high temperature. The reason for that may be attributed to the agglomeration of particles. The maximum enhancement of thermal conductivity for CNT-AL₂O₃ nanofluid was 2.7% recorded for a weight concentration of 0.5 % at 40°C.

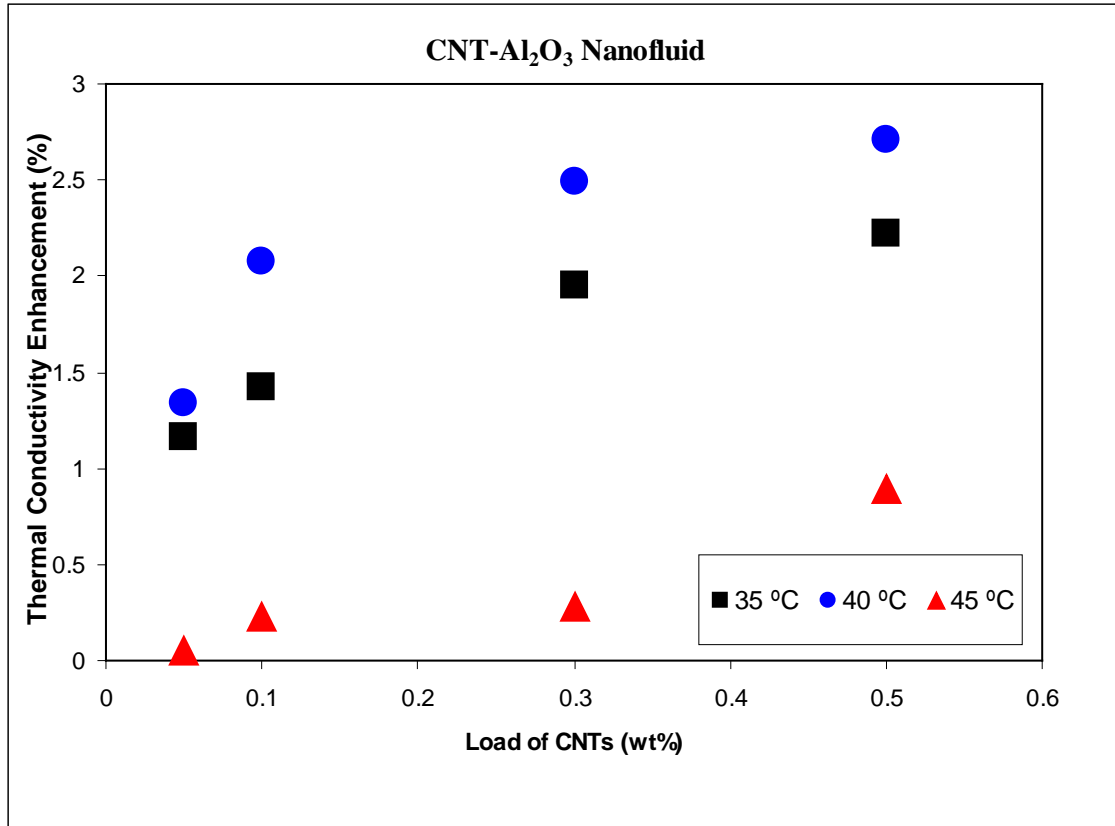


Figure 4.19 Thermal conductivity enhancement of DI water with CNT- Al_2O_3 nanofluid

4.4.1.4 Effect of Concentration on Thermal Conductivity for DI water+CNT-CuO Nanofluid

Figure 4.20 shows the enhancement of thermal conductivity for nanofluid of CNT-CuO with deionized water. The load of metal oxide fixed at 10 wt % of CNT. The thermal conductivities of this nanofluid have been measured at weight fractions of 0.05%, 0.1%, 0.3% and 0.5% for different temperatures. From the experimental results, it is clearly shown that, the thermal conductivity enhancement increased with increasing nanoparticles weight concentration. Also, it is found that, the thermal conductivity enhancement increased with increasing temperature but decreased at high temperature. The maximum enhancement of thermal conductivity for CNT-CuO nanofluid was 3.1% recorded for a weight concentration of 0.5% at 40°C.

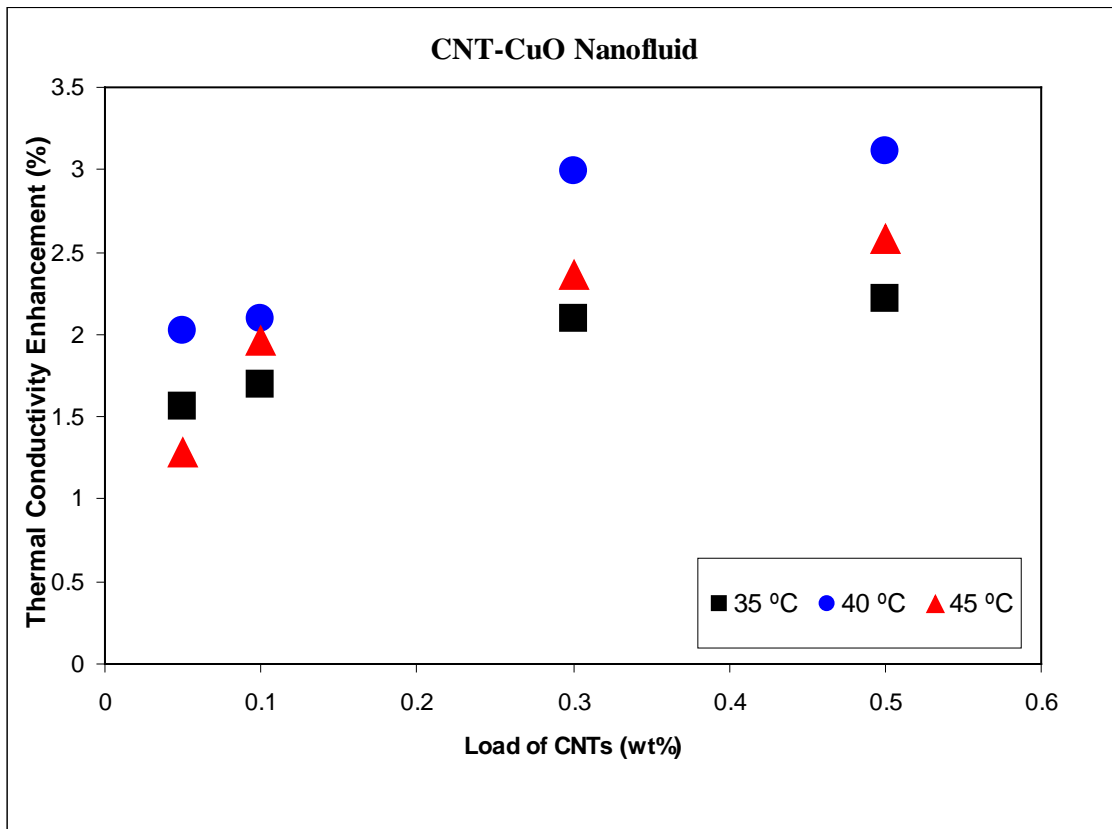


Figure 4.20 Thermal conductivity enhancement of DI water and CNT-CuO nanofluid

4.5 Application of CNT-PEG Nanofluid in Heat Exchanger

In this section, the performance of a concentric tube heat exchanger has been experimentally investigated in terms of effectiveness calculations. It was found from the previous sections that, the CNT-PEG nanofluid has to be able to produce a stable nanofluid with deionized water for more than two months without visually observable precipitation. Also, CNT-PEG nanofluid shows more enhancements in thermal conductivity compared to the other tested nanofluids.

Based on these findings, the effectiveness calculations of the concentric tube heat exchanger using CNT-PEG nanofluid have been conducted at weight fractions of 0.05%, 0.1% and 0.2% under turbulent and laminar conditions. The heat exchanger consisted of 1.59 m annular tube which was constructed of 13.5 mm diameter inner copper tube with 1.25 mm thickness and 22.5 mm diameter outer glass tube.

The experimental results show that, the use of CNT-PEG nanofluid was enhanced the effectiveness of the heat exchanger in the turbulent regime at $Re = 5800$. The enhancement increased with particles weight concentration under the condition of experiments as shown in Figure 4.21. The maximum enhancement of effectiveness for CNT-PEG nanofluid was around 25% observed for a particle concentration of 0.2 wt %.

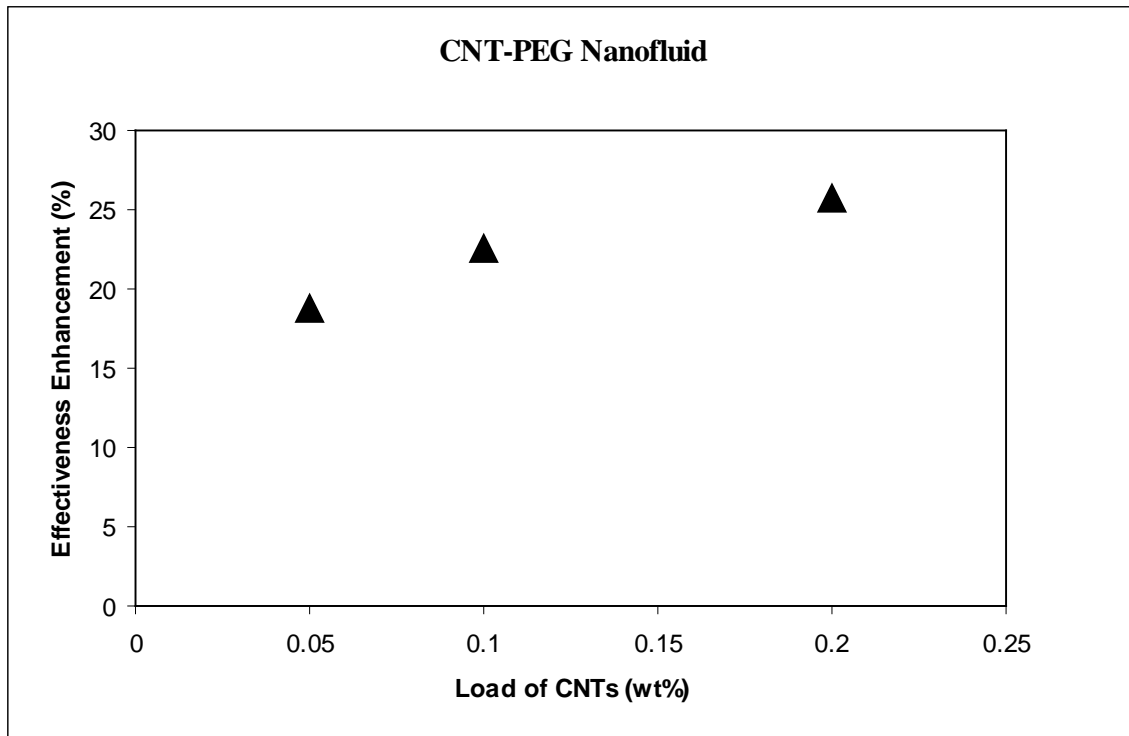


Figure 4.21 Effectiveness enhancement of CNT-PEG nanofluid in the turbulent regime

The reasons for the effectiveness enhancement by CNT-PEG nanofluid may be attributed to the increasing in heat transfer coefficient due to the increasing in thermal conductivity since $h \propto k/\delta$, and due to the decreased thermal boundary layer thickness due to non-uniform distribution of thermal conductivity and viscosity resulting from Brownian motion of nanoparticles [35].

Where:

h : Heat transfer coefficient

k : Thermal conductivity

δ : Thickness of the thermal boundary layer

Figure 4.22 exhibits effectiveness enhancements of CNT-PEG nanofluid in laminar flow at $Re = 2100$. It can be seen that, there is no clear trend. The maximum enhancement of effectiveness was around 54% observed for 0.2 wt % particle concentration. Because CNT-PEG nanofluid has black color, the float of flow meter can not be seen clearly. In case of turbulent flow, fully open flow was tested but in case of laminar flow digital flow meter should be used.

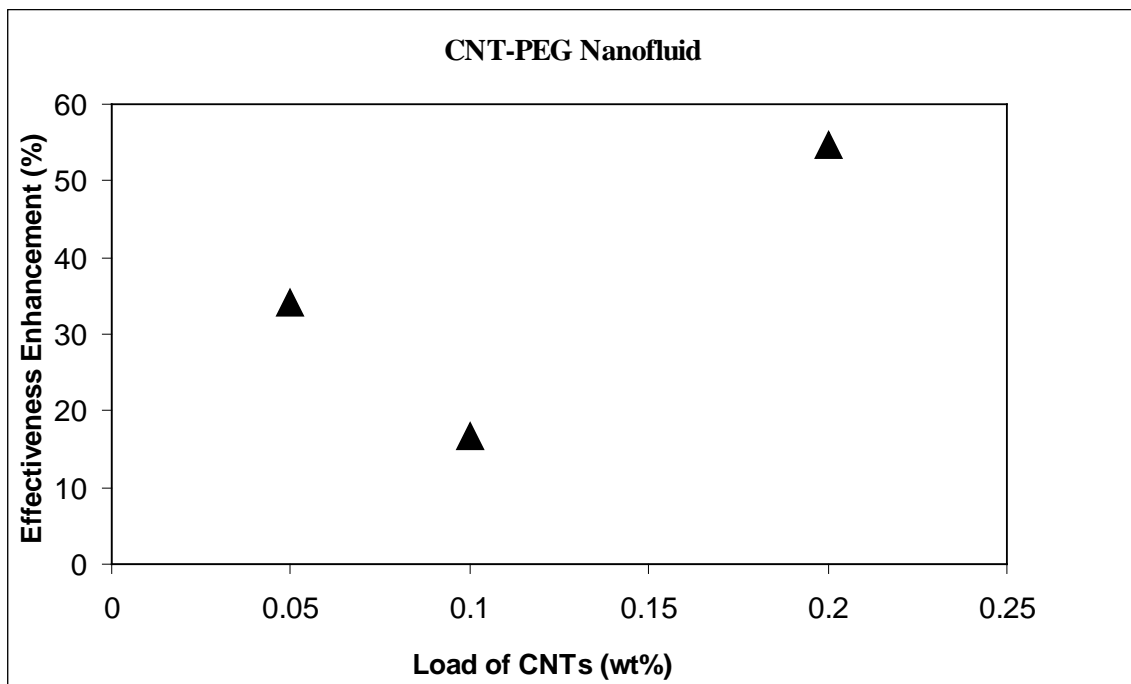


Figure 4.22 Effectiveness enhancement of CNT-PEG nanofluid in the laminar regime

From these results, it can be said that the use of CNT-PEG nanofluid was increased the ability of the concentric tube heat exchanger to exchange the temperatures between the fluids. Consequently, the size of heat exchanger may be reduced in industrial process and energy can be saved by using CNT-PEG nanofluid.

CHAPTER FIVE

5 CONCLUSIONS AND RECOMMENDATIONS

5.1 *Conclusions*

Based on experimental findings, it was found that, oxidized MWCNTs and MWCNTs-PEG were found to be able to prepare a stable nanofluid with deionized water for more than two months without visually observable precipitation, while MWCNTs-Amine nanofluid showed quick CNT precipitation. Functionalized carbon nanotubes with octadecanol and phenol failed to produce stable and homogeneous suspensions with water.

Impregnated carbon nanotubes with copper oxide (CuO) and aluminum oxide (Al₂O₃) allowed stable and homogenous nanofluids preparation with water in presence of sodium dodecyl- sulfate (SDS) as a dispersing agent.

Nanofluids containing carbon nanotubes functionalized with oxygen containing functional groups showed more enhancements of thermal conductivity in comparison to nanofluids containing impregnated carbon nanotubes with metal oxides. The maximum enhancement of thermal conductivity was around 4% in case of MWCNTs-PEG nanofluid for 0.5 wt % particle concentration. The impregnated carbon nanotubes were agglomerated and formed large particles. The thermal conductivity enhancement decreased at high temperature. The cause may be attributed to the agglomeration of nanoparticles.

Nanofluid of deionized water and functionalized carbon nanotubes with poly-ethylene glycol has a promising future to be used as an effective heat transfer fluid. In this study, the performance of the concentric tube heat exchanger was improved by using MWCNTs-PEG nanofluid and it is found from the experiments that, the effectiveness enhancement in turbulent regime increased with increasing particles weight concentration reaching to around 25% for 0.2 wt % particle concentration. In case of laminar flow, there is no a clear trend. The maximum enhancement of effectiveness was around 54% observed for 0.2 wt % particle concentration.

The effectiveness enhancement of heat exchanger could not be only attributed to the thermal conductivity enhancement. Migration of particles and Brownian motion of nanoparticles may be proposed to be reasons for the enhancement which cause a non-uniform distribution of the thermal conductivity and viscosity and decreases the thickness of the boundary layer.

5.2 Recommendations

Based on the results of this study, the following recommendations are made to improve the quality of the data and to extend the scope of the research area:

1. Use ethylene glycol as a base fluid instead of water and study the effects of MWCNT-PEG concentration on the thermal conductivity and effectiveness of heat exchangers.
2. Simulate the nanofluid flow in a concentric tube heat exchanger using suitable package such as computational fluid dynamics (CFD).

APPENDIXE

APPENDIX A

Thermal Properties of CNT-Nanofluids

Table A4. 1 Thermal properties of CNT-COOH nanofluid at 35°C

Weight Fraction (%)	Effusivity ($Ws^{1/2}/m^2/K$)	Thermal Conductivity (W/m K)	Heat Capacity (J/kg/K)
0.00	1607	0.6217	4175
0.05	1625	0.6296	4215
0.1	1628	0.6311	4220
0.3	1649	0.6404	4267
0.5	1653	0.6425	4274

Table A4. 2 Thermal properties of CNT-COOH nanofluid at 40°C

Weight Fraction (%)	Effusivity ($Ws^{1/2}/m^2/K$)	Thermal Conductivity (W/m K)	Heat Capacity (J/kg/K)
0.00	1614	0.6247	4204
0.05	1643	0.6378	4267
0.1	1645	0.6389	4270
0.3	1651	0.6414	4284
0.5	1655	0.6435	4291

Table A4. 3 Thermal properties of CNT-COOH nanofluid at 45°C

Weight Fraction (%)	Effusivity ($Ws^{1/2}/m^2/K$)	Thermal Conductivity (W/m K)	Heat Capacity (J/kg/K)
0.00	1644	0.6386	4275
0.05	1658	0.6446	4308
0.1	1659	0.6450	4310
0.3	1663	0.6469	4318
0.5	1683	0.6560	4361

Table A4. 4 Thermal properties of CNT-PEG nanofluid at 35°C

Weight Fraction (%)	Effusivity ($Ws^{1/2}/m^2/K$)	Thermal Conductivity (W/m K)	Heat Capacity (J/kg/K)
0.00	1607	0.6217	4175
0.05	1619	0.6296	4184
0.1	1633	0.6333	4233
0.3	1649	0.6405	4267
0.5	1663	0.6469	4297

Table A4. 5 Thermal properties of CNT-PEG nanofluid at 40°C

Weight Fraction (%)	Effusivity ($Ws^{1/2}/m^2/K$)	Thermal Conductivity (W/m K)	Heat Capacity (J/kg/K)
0.00	1614	0.6247	4204
0.05	1649	0.6404	4280
0.1	1654	0.6430	4289
0.3	1656	0.6435	4296
0.5	1666	0.6482	4316

Table A4. 6 Thermal properties of CNT-PEG nanofluid at 45°C

Weight Fraction (%)	Effusivity ($Ws^{1/2}/m^2/K$)	Thermal Conductivity (W/m K)	Heat Capacity (J/kg/K)
0.00	1644	0.6386	4275
0.05	1654	0.6430	4298
0.1	1661	0.6459	4315
0.3	1662	0.6462	4318
0.5	1686	0.6575	4367

Table A4. 7 Thermal properties of CNT-10%CuO nanofluid at 35°C

Weight Fraction (%)	Effusivity ($Ws^{1/2}/m^2/K$)	Thermal Conductivity (W/m K)	Heat Capacity (J/kg/K)
0.00	1607	0.6217	4175
0.05	1629	0.6314	4224
0.1	1631	0.6322	4227
0.3	1636	0.6348	4237
0.5	1638	0.6355	4242

Table A4. 8 Thermal properties of CNT-10%CuO nanofluid at 40°C

Weight Fraction (%)	Effusivity ($Ws^{1/2}/m^2/K$)	Thermal Conductivity (W/m K)	Heat Capacity (J/kg/K)
0.00	1614	0.6247	4204
0.05	1642	0.6373	4265
0.1	1643	0.6378	4267
0.3	1655	0.6434	4291
0.5	1657	0.6441	4296

Table A4. 9 Thermal properties of CNT-10%CuO nanofluid at 45°C

Weight Fraction (%)	Effusivity ($Ws^{1/2}/m^2/K$)	Thermal Conductivity (W/m K)	Heat Capacity (J/kg/K)
0.00	1644	0.6386	4275
0.05	1663	0.6468	4319
0.1	1672	0.6511	4338
0.3	1678	0.6537	4351
0.5	1681	0.6551	4357

Table A4. 10 Thermal properties of CNT-10%Al₂O₃ nanofluid at 35°C

Weight Fraction (%)	Effusivity (Ws^{1/2}/ m² /K)	Thermal Conductivity (W/m K)	Heat Capacity (J/kg/K)
0.00	1607	0.6217	4175
0.05	1623	0.6289	4212
0.1	1627	0.6305	4219
0.3	1634	0.6338	4234
0.5	1638	0.6355	4243

Table A4. 11 Thermal properties of CNT-10%Al₂O₃ nanofluid at 40°C

Weight Fraction (%)	Effusivity (Ws^{1/2}/ m² /K)	Thermal Conductivity (W/m K)	Heat Capacity (J/kg/K)
0.00	1614	0.6247	4204
0.05	1633	0.6331	4244
0.1	1643	0.6377	4267
0.3	1648	0.6402	4276
0.5	1651	0.6416	4285

Table A4. 12 Thermal properties of CNT-10%Al₂O₃ nanofluid at 45°C

Weight Fraction (%)	Effusivity (Ws^{1/2}/ m² /K)	Thermal Conductivity (W/m K)	Heat Capacity (J/kg/K)
0.00	1644	0.6386	4275
0.05	1645	0.6389	4281
0.1	1648	0.6401	4286
0.3	1649	0.6404	4289
0.5	1657	0.6443	4306

Experimental calculated values for Effectiveness Calculations of Heat Exchanger

Temperature of heating unit = 40 °C

Temperature of cooling unit = 20 °C

Table A4. 13 Experimental and calculated values for effectiveness calculations for water/water system

Parameter	Hot Fluid	Cold Fluid
Inlet temperature (in °C)	38	21.5
Outlet temperature (in °C)	34.9	26.6
Specific heat at average temperature (in J/kg .K)	4178	4181
Mass flow rate (in kg/s)	0.04303	0.0253
Heat Capacity rate, $m \cdot C_p$ (in W/K)	179.8	105.8
Heat transfer rate , $q = m \cdot C_p T_{in} - T_{out} $ (in W)	557	
Maximum possible heat transfer, $q_{max} (m \cdot C_p)_{min} (T_{h,in} - T_{c,in})$ (in W)	1746	
Heat exchanger effectiveness, $\epsilon = q/q_{max}$	0.319	
Parameter	Hot Fluid	Cold Fluid
Inlet temperature (in °C)	37.6	20.8
Outlet temperature (in °C)	33.6	24
Specific heat at average temperature (in J/kg .K)	4178	4181
Mass flow rate (in kg/s)	0.01655	0.0253
Heat Capacity rate, $m \cdot C_p$ (in W/K)	69.15	105.8
Heat transfer rate , $q = m \cdot C_p T_{in} - T_{out} $ (in W)	277	
Maximum possible heat transfer, $q_{max} (m \cdot C_p)_{min} (T_{h,in} - T_{c,in})$ (in W)	1162	
Heat exchanger effectiveness, $\epsilon = q/q_{max}$	0.238	

Table A4. 14 Experimental and calculated values for effectiveness calculations for 0.05 % CNT-PEG nanofluid in tube side and water in shell side

Parameter	Hot Fluid	Cold Fluid
Inlet temperature (in °C)	38	21.5
Outlet temperature (in °C)	34.9	26.6
Specific heat at average temperature (in J/kg .K)	4178	4181
Mass flow rate (in kg/s)	0.04303	0.0253
Heat Capacity rate, $m \cdot C_p$ (in W/K)	179.8	105.8
Heat transfer rate , $q = m \cdot C_p T_{in} - T_{out} $ (in W)	557	
Maximum possible heat transfer, $q_{max} (m \cdot C_p)_{min} (T_{h, in} - T_{c, in})$ (in W)	1746	
Heat exchanger effectiveness, $\epsilon = q/q_{max}$	0.319	
Parameter	Hot Fluid	Cold Fluid
Inlet temperature (in °C)	37.6	20.8
Outlet temperature (in °C)	33.6	24
Specific heat at average temperature (in J/kg .K)	4178	4181
Mass flow rate (in kg/s)	0.01655	0.0253
Heat Capacity rate, $m \cdot C_p$ (in W/K)	69.15	105.8
Heat transfer rate , $q = m \cdot C_p T_{in} - T_{out} $ (in W)	277	
Maximum possible heat transfer, $q_{max} (m \cdot C_p)_{min} (T_{h, in} - T_{c, in})$ (in W)	1162	
Heat exchanger effectiveness, $\epsilon = q/q_{max}$	0.238	

Table A4. 15 Experimental and calculated values for effectiveness calculations for 0.1 % CNT-PEG nanofluid in tube side and water in shell side

Parameter	Hot Fluid	Cold Fluid
Inlet temperature (in °C)	38	21.5
Outlet temperature (in °C)	34.9	26.6
Specific heat at average temperature (in J/kg .K)	4178	4181
Mass flow rate (in kg/s)	0.04303	0.0253
Heat Capacity rate, $m \cdot C_p$ (in W/K)	179.8	105.8
Heat transfer rate , $q = m \cdot C_p T_{in} - T_{out} $ (in W)	557	
Maximum possible heat transfer, $q_{max} (m \cdot C_p)_{min} (T_{h, in} - T_{c, in})$ (in W)	1746	
Heat exchanger effectiveness, $\epsilon = q/q_{max}$	0.319	
Parameter	Hot Fluid	Cold Fluid
Inlet temperature (in °C)	37.6	20.8
Outlet temperature (in °C)	33.6	24
Specific heat at average temperature (in J/kg .K)	4178	4181
Mass flow rate (in kg/s)	0.01655	0.0253
Heat Capacity rate, $m \cdot C_p$ (in W/K)	69.15	105.8
Heat transfer rate , $q = m \cdot C_p T_{in} - T_{out} $ (in W)	277	
Maximum possible heat transfer, $q_{max} (m \cdot C_p)_{min} (T_{h, in} - T_{c, in})$ (in W)	1162	
Heat exchanger effectiveness, $\epsilon = q/q_{max}$	0.238	

Table A4. 16 Experimental and calculated values for effectiveness calculations for 0.2 % CNT-PEG nanofluid in tube side and water in shell side

Parameter	Hot Fluid	Cold Fluid
Inlet temperature (in °C)	38	21.5
Outlet temperature (in °C)	34.9	26.6
Specific heat at average temperature (in J/kg .K)	4178	4181
Mass flow rate (in kg/s)	0.04303	0.0253
Heat Capacity rate, $m \cdot C_p$ (in W/K)	179.8	105.8
Heat transfer rate , $q = m \cdot C_p T_{in} - T_{out} $ (in W)	557	
Maximum possible heat transfer, $q_{max} (m \cdot C_p)_{min} (T_{h, in} - T_{c, in})$ (in W)	1746	
Heat exchanger effectiveness, $\epsilon = q/q_{max}$	0.319	
Parameter	Hot Fluid	Cold Fluid
Inlet temperature (in °C)	37.6	20.8
Outlet temperature (in °C)	33.6	24
Specific heat at average temperature (in J/kg .K)	4178	4181
Mass flow rate (in kg/s)	0.01655	0.0253
Heat Capacity rate, $m \cdot C_p$ (in W/K)	69.15	105.8
Heat transfer rate , $q = m \cdot C_p T_{in} - T_{out} $ (in W)	277	
Maximum possible heat transfer, $q_{max} (m \cdot C_p)_{min} (T_{h, in} - T_{c, in})$ (in W)	1162	
Heat exchanger effectiveness, $\epsilon = q/q_{max}$	0.238	

REFERENCES

- [1] Marquis, F.D.S and Chibante, L.P.F., *Improving the heat transfer of nanofluids and nanolubricants with carbon nanotubes*, JOM (2005), 32–43.
- [2] Y. Li, J. Zhou, S. Tung, E., Schneider and S. Xi., *A review on development of nanofluid preparation and characterization*, Powder Technol. 196 (2009), 89-101.
- [3] J.A. Eastman, S.U.S. Choi, *Anomalously increased effective thermal conductivities of ethylene glycol-based nanofluids containing copper nanoparticles*, Appl. Phys. Lett. 78 (2001) 718–720.
- [4] Min-Sheng Liu, MarkChing-Cheng Lin, C.Y. Tsai, Chi-Chuan Wang, *Enhancement of thermal conductivity with cu for nanofluids using chemical reduction method*, Int. J. Heat Mass Transfer 49 (2006) 3028–3033.
- [5] C.H. Lo, T.T. Tsung, L.C. Chen, C.H. Su, H.M. Lin, *Fabrication of copper oxide nanofluid using submerged arc nanoparticle synthesis system (SANSS)*, J. Nanopart. Res. 7 (2005) 313–320.
- [6] C.H. Lo, T.T. Tsung, L.C. Chen, *Shape-controlled synthesis of Cu-based Nanofluid using submerged arc nanoparticle synthesis system (SANSS)*, J. Cryst. Growth 277 (2005) 636–642.
- [7] H. Zhu, Y. Lin, Y. Yin, *A novel one-step chemical method for preparation of copper nanofluids*, J. Colloid Interface Sci. 227 (2004) 100–103.
- [8] M.S. Liu, M.C. Lin, I.Te. Huang, C.C. Wang, *Enhancement of thermal conductivity with carbon nanotube for nanofluids*, Int. Commun. Heat Mass Transf. 32 (2005) 1202–1210.

- [9] S.U.S. Choi, Z.G. Zhang, W. Yu, F.E. Lockwood, E.A. Grulke, *Anomalous thermal conductivity enhancement in nanotube suspensions*, Appl. Phys. Lett. 79 (2001) 2252–2254.
- [10] T.K. Hong, H.S. Yang, C.J. Choi, *Study of the enhanced thermal conductivity of Fe nanofluids*, J. Appl. Phys. 97 (064311) (2005) 1–4.
- [11] K.S. Hong, T.K. Hong, H.S. Yang, *Thermal conductivity of Fe nanofluids depending on the cluster size of nanoparticles*, Appl. Phys. Lett. 88 (31901) (2006) 1–3.
- [12] Y. Xuan, Q. Li, *Heat transfer enhancement of nanofluids*, Int. J. Heat Mass Transfer 21 (2000) 58–64.
- [13] Q. Li, Y. Xuan, *The heat conduction properties of fluxion and convective of Cu/H₂O nanofluids*, Sci. China, Ser. E 32 (2002) 331–337 (in chinese).
- [14] Y. Xuan, Q. Li, *Heat transfer enhancement of nanofluids*, J. Eng. Thermophys. 21 (2000) 466–470 (in Chinese).
- [15] S.M.S. Murshed, K.C. Leong, C. Yang, *Enhanced thermal conductivity of TiO₂-water based nanofluid*, Int. J. Therm. Sci. 44 (2005) 367–373.
- [16] H. Xie, J. Wang, T. Xi, Y. Liu, F. Ai, *Thermal conductivity enhancement of suspensions containing nanosized alumina particle*, J. Appl. Phys. 91 (2002) 4568–4572.
- [17] Lee, S., Choi, U.S., Li, S., and Eastman, J.A., 1999, *Measuring thermal conductivity of fluids containing oxide nanoparticles*, Journal of Heat transfer, 121 (1999), 280–289.
- [18] Eastman, J. A., Choi, U. S., Li, S., Yu, W., and Thompson, L. J., *Anomalously increased effective thermal conductivities of ethylene glycol-based nanofluids containing copper nanoparticles*, Appl. Phys. Lett., 78(14) (2001), 718–720.

- [19] Choi, S.U.S., Z.G. Zhang, W. Yu, F.E. Lockwood & E.A. Grulke, *Anomalous thermal conductivity enhancement in nanotube suspension*, Appl. Phys. Lett. 79(14) (2001), 2252–2254.
- [20] M.J. Assael, C.F. Chen, I.N. Metaxa, W.A. Wakeham, *Thermal conductivity of suspensions of carbon nanotubes in water*, International Journal of Thermophysics 25 (4) (2004) 971–985.
- [21] Assael, M. J., Metaxa, I. N., Arvanitidis, J., Christophilos, D., and Lioutas, C., *Thermal conductivity enhancement in aqueous suspensions of carbon multi-walled and double-walled Nanotubes in the presence of two different dispersants*, International Journal of Thermophysics, 26 (3) (2005), 647–664.
- [22] M.S. Liu, M.C.C. Lin, I.T. Huang, C.C. Wang, *Enhancement of thermal conductivity with carbon nanotube for nanofluids*, Int. Commun. Heat Mass Transfer 32 (2005) 1202–1210.
- [23] Y.J. Hwang, Y.C. Ahn, H.S. Shin, C.G. Lee, G.T. Kim, H.S. Park, J.K. Lee, *Investigation on characteristics of thermal conductivity enhancement of nanofluids*, Current Applied Physics 6 (2006) 1068–1071.
- [24] Yulong Ding, Haisheng Chen, Liang Wang, Chane-Yuan Yang, Yurong He, Wei Yang, WaiPeng Lee, Lingling Zhang, Ran Huo, *Heat transfer intensification using nanofluids*, KONA 25 (2007).
- [25] Xue Q Z , *Model for thermal conductivity of carbon nanotube-based composites* , Physica B: Condensed Matter, 368 (2005), 302–307.
- [26] Nan CW, Shi Z, Lin Y, *A simple model for thermal conductivity of carbon nanotube-based composites*, Chem Phys Lett, 375(2003) 666–669.

- [27] Nan CW, Liu G, Lin YH, Li M, *Interface effect on thermal conductivity of carbon nanotube composites*, Appl Phys Lett,85(2004) 3549–3551.
- [28] L. Gao, X.F. Zhou, *Differential effective medium theory for thermal conductivity in nanofluids*, Phys. Lett. A, 348 (2006) 355–360.
- [29] Pak, B.C. and Young, C.I., *Hydrodynamic and heat transfer study of dispersed fluids with submicron metallic oxide particles*, Exp. Heat Transfer, 11 (1998), 151–170.
- [30] Eastman, J.A., Choi, U.S., Li. S., Soyez, G., Thompson, L.J. and DiMelfi, R.J., *Novel thermal properties of nanostructure materials*, Mater. Sci. Forum, 312 (1999), 629–634.
- [31] Xuan, Y.and Qiang, Li. *Investigation on convective heat transfer and flow features of nanofluids*, J.Heat Transfer, 125 (2003), 151–155.
- [32] Wen ,D.and Ding, Y., *Experimental investigation into convective heat transfer of nanofluids at the entrance region under laminar flow conditions*, Int. J. Heat Mass Transfer, 47 (2004), 5181–5188.
- [33] Ding, Y., Alias, H., Wen, D. and Williams, R.A., *Heat transfer of aqueous suspensions of carbon nanotubes(CNT nanofluids)*, Int. J. Heat Mass Transfer, 49 (2006), 240–250.
- [34] Yang, Y., Zhang, Z.G.; Grulke, E.A., Anderson, W.B. and Wu, G., *Heat transfer properties of nanoparticles-in-fluid dispersions (nanofluids) in laminar flow*, Int. J. Heat Mass Transfer, 48 (2005), 1107–1116.
- [35] Heris, Zeinali S., Esfahany, Nasr M., Etemad, S.G., *Experimental investigation of convective heat transfer of Al₂O₃/water nanofluid in circular tube*, Int. J. Heat Fluid Flow, 28 (2007), 203–210.

- [36] Asirvatham, L., Vishal, N., Gangatharan, S., Lal, D., *Experimental study on forced convective heat transfer with low volume fraction of CuO/Water nanofluid*, *Energies*, 2 (2009), 97–119.
- [37] Faraj A. Abuilawi, Tahar Laoui, Mamdouh Al-Harhi, and Muataz Ali Atieh, *Modification and functionalization of multiwalled carbon nanotube (MWCNT) via Fischer Esterification*, *The Arabian Journal for Science and Engineering*, June 2010, Volume 35, Number 1C.
- [38] Abdelghani Laachachi, Alexander Vivet, Gerad Nouet, Bessem Ben Doudou, Christophe Poilane, Jun Chen, Jin Bo bai, M'Hamed Ayachi, *A chemical method to graft carbon nontubes onto a carbon fiber*, *Materials Letters*, 62 (2008), 394.
- [39] San Ping Jiang, *A review of wet impregnation—An alternative method for the fabrication of high performance and nano-structured electrodes of solid oxide fuel cells*, *Materials Science and Engineering A.*, 418 (2006) 199–210
- [40] da Silva-Neto ID, *Improvement of silver impregnation technique (protargol) to obtain morphological features of protists, ciliates, flagellates and opalينات*, *Rev Bras Biol* 60(3) 2000, 451–459.
- [41] R. Williams, *Spectroscopy and the Fourier Transform: an interactive tutorial*, VCH Publishers Inc., (1996), 7–9.
- [42] C. Branca, F. Frusteri, V. Magazu, and A. Mangione, *Characterization of carbon nanotubes by TEM and infrared spectroscopy*, *J. Phys. Chem. B* ,108 (2004) 3469–3473
- [43] www.siliconfareast.com
- [44] A. Harris and D.N. Sorensen, *Thermal conductivity testing of minimal volumes of energetic powders*, *Journal of Pyrotechnics*, 25, 2007.

- [45] Frank P. Incropera, David P. DeWitt, Theodore L. Bergman, Adrienne S. Lavine, *Fundamentals of heat and mass transfer*, 6th-Edition, Publisher: Wiley, (2006).
- [46] W. Zhang, J.K. Sprafke, M.A. Minglin, E.Y. Tsui, S.A. Sydlík, G.C. Rutledge, T.M. Swager, *Modular functionalization of carbon nanotubes and fullerenes*, *J. Amer. Chem. Soc.*, 131(2009), 8446–8454.
- [47] J. Kathi, K. Rhee, J. Lee, *Effect of chemical functionalization of multiwalled carbon nanotubes with 3-aminopropyltriethoxysilane on mechanical and morphological properties of epoxy nanocomposites*, *Composites*, 40(2009), 800–809.
- [48] I. Belinda, Rosario-castro, Enid J. Contes, Marisabel Lebron-Colon, Micheal A. Meador, Germarie Sanchez-pomales, carlosr Cabrera, *Combined electro microscopy and spectroscopy characterization of as-received, acid purified and oxidized hiPCO single-wall carbon nanotubes*, *Material characterization*, 60(2009), 1442–1453.
- [49] Z. Dang, L. Wang, L. Zhang, *Surface functionalization of multiwalled carbon nanotubes with trifluorophenyl*, *Journal of Nanomaterials*, 2006, 1–5.
- [50] Z. Liu, Y. Xu, X. Zhang, Y. Chan, J. Tian, *Porphyrin and fullerene covalently functionalized graphene hybrid materials with large nonlinear optical properties*, *J. Phys. Chem. B.*, 113(2009), 9681–9686.
- [51] G. Ovejero, J. L. Sotelo, M. D. Romero, A. Rodríguez, M. A. Ocana, G. Rodríguez, and J. Garcia, *Multiwalled carbon nanotubes for liquid-Phase oxidation. Functionalization, characterization, and catalytic activity*, *Ind. Eng. Chem. Res.*, 45(2006), 2206–2212.
- [52] Z. Zhang, F.E. Lockwood, *Preparation of stable nanotubes dispersions in liquids*, US Patent US6783746B1, August 31, 2004.

VITAE

NAME: Osamah Awadh Khamis Bin Dahman

NATIONALITY: Yemeni

EDUCATIONAL QUALIFICATIONS:

Master of Science in Chemical Engineering

Sept. 2007 – June 2011

King Fahd University of Petroleum and Minerals, Dhahran, Saudi Arabia

Bachelor of Science in Chemical Engineering

Sept. 1998 – June 2003 Hadhramout University of science and technology,

Al Mukalla, Yemen

First of the department of chemical engineering (2003)

E-MAIL ADDRESS: osamaawad78@hotmail.com

PRESENT ADDRESS: Building 829, Room 105

KFUPM, Dhahran Saudi Arabia

PERMANENT ADDRESS: Hadhramout-Yemen